CO_2 MINIMUM MISCIBILITY PRESSURE AND RECOVERY MECHANISMS IN HETEROGENEOUS LOW PERMEABILITY RESERVOIRS

Kaiyi Zhang

Thesis submitted to the faculty of the Virginia Polytechnic Institute and State University in partial fulfillment of the requirements for the degree of

Master of Science
In
Mining Engineering

Bahareh Nojabaei, Chair

Nino S. Ripepi
Jonathan B. Boreyko

August 7, 2019
Blacksburg, VA

Keywords: Pore Confinement Effect, Gas-oil Capillary Pressure, CO_2 Injection, Minimum Miscibility Pressure, Shale Nano-pore, Pore Size Heterogeneity, Molecular Diffusion

CO_2 MINIMUM MISCIBILITY PRESSURE AND RECOVERY MECHANISMS IN HETEROGENEOUS LOW PERMEABILITY RESERVOIRS

Kaiyi Zhang

ACADEMIC ABSTRACT

Benefiting from the efficiency of hydraulic fracturing and horizontal drilling, the production of unconventional oil and gas resources, such as shale gas and tight oil, has grown quickly in 21st century and contributed to the North America oil and gas production. Although the new enhancing oil recovery (EOR) technologies and strong demand spike the production of unconventional resources, there are still unknowns in recovery mechanisms and phase behavior in tight rock reservoirs. In such environment, the phase behavior is altered by high capillary pressure owing to the nanoscale pore throats of shale rocks and it may also influence minimum miscibility pressure (MMP), which is an important parameter controlling gas floods for CO_2 injection EOR. To investigate this influence, flash calculation is modified with considering capillary pressure and this work implements three different methods to calculate MMP: method of characteristics (MOC); multiple mixing cell (MMC); and slim-tube simulation. The results show that CO_2 minimum miscibility pressure in nanopore size reservoirs are affected by gas-oil capillary pressure owing to the alteration of key tie lines in displacement. The values of CO_2-MMP from three different methods match well.

Moreover, in tight rock reservoirs, the heterogeneous pore size distribution, such as the ones seen in fractured reservoirs, may affect the recovery mechanisms and MMP. This work also investigates the effect of pore size heterogeneity on multicomponent multiphase hydrocarbon fluid composition distribution and its subsequent influence on mass transfer through shale nanopores. According to the simulation results, compositional gradient forms in heterogeneous nanopores of tight reservoirs because oil and gas phase compositions depend on the pore size. Considering that permeability is small in tight rocks and shales, we expect that mass transfer

within heterogeneous pore size porous media to be diffusion-dominated. Our results imply that there can be a selective matrix-fracture component mass transfer during both primary production and gas injection secondary recovery in fractured shale rocks. Therefore, molecular diffusion should not be neglected from mass transfer equations for simulations of gas injection EOR or primary recovery of heterogeneous shale reservoirs with pore size distribution.

CO_2 MINIMUM MISCIBILITY PRESSURE AND RECOVERY MECHANISMS IN HETEROGENEOUS LOW PERMEABILITY RESERVOIRS

Kaiyi Zhang

GENERAL AUDIENCE ABSTRACT

The new technologies to recover unconventional resources in oil and gas industry, such as fracturing and horizontal drilling, boosted the production of shale gas and tight oil in 21st century and contributed to the North America oil and gas production. Although the new technologies and strong demand spiked the production of tight oil resources, there are still unknowns of oil and gas flow mechanisms in tight rock reservoirs. As we know, the oil and gas resources are stored in the pores of reservoir formation rock. During production process, the oil and gas are pushed into production wells by formation pressure. However, the pore radius of shale rock is extremely small (around nanometers), which reduces the flow rate of oil and gas and raises capillary pressure in pores. The high capillary pressure will alter the oil and gas phase behavior and it may influence the value of minimum miscibility pressure (MMP), which is an important design parameter for CO_2 injection (an important technology to raise production). To investigate this influence, we changed classical model with considering capillary pressure and this modified model is implemented in different methods to calculate MMP. The results show that CO_2-MMP in shale reservoirs are affected by capillary pressure and the results from different methods match well.

Moreover, in tight rock reservoirs, the heterogeneous pore size distribution, such as fractures in reservoirs, may affect the flow of oil and gas and MMP value. So, this work also investigates the effect of pore size heterogeneity on oil and gas flow mechanisms. According to the simulation results, compositional gradient forms in heterogeneous nanopores of tight reservoirs and this gradient will cause diffusion which will dominate the other fluid flow mechanisms. Therefore, we always need to consider molecular diffusion in the simulation model for shale reservoirs.

ACKNOWLEDGMENTS

First of all, I would like to express my sincere gratitude to my advisor Dr. Bahareh Nojabaei for her unconditional support and patience to help me overcoming numerous difficulties I have been facing through my research and this work is also funded by her research foundation. This work would not be done without her support and I could not imagine having a better mentor in my master study. Thank you for being the enlightener on my academic path.

Besides my advisor, I would like to acknowledge the rest number of my committee Dr. Jonathan Boreyko and Dr. Nino Ripepi for their constructive comments and encouragement to help finish my thesis.

Also my sincere thanks goes to Dr. Kaveh Ahmadi and Dr. Nithiwat Siripatrachai who provided me opportunity to join their team as intern and helping me landing my research on real industrial problems.

I would like to thank my research partner Fengshuang Du who is a Ph.D. candidate in our group for helping me polish my papers and I will miss our daily discussions of any ideas and questions we came up with.

Last but not the least, I would like to thank my parents and Yuxiao Shi for their spiritual support throughout my research and my life for years.

TABLE OF CONTENTS

LIST OF FIGURES

LIST OF TABLES

Introduction

This thesis includes three main chapters, which investigates the effect of high capillary pressure on the CO_2 minimum miscibility pressure (MMP) and recovery mechanism of petroleum fluids in tight reservoirs with heterogeneous pore size distribution. In the nanopore confined space, like the ones in shale, the oil and gas phase behavior will be influenced by large gas-oil capillary pressure. Therefore, all these studies are based on the theory of effect of high capillary pressure on phase behavior of hydrocarbon fluid. In this research study, simulation model is modified with effect of capillary pressure to model the fluid flow and phase behavior in nanopores confined space. This model is implemented in the following two research studies in following chapters of this thesis and can be applied to any simulation projects in tight rocks.

In Chapter.1, the nanopore confinement effect on CO_2-MMP is investigated, and it is concluded that the value of multiple contact MMP in tight reservoir are influenced by high capillary pressure. This research includes three different methods to calculate MMP, which are slim-tube simulation; method of characteristics and multiple mixing cell method. Real shale reservoir fluids (Bakken, Eagle Ford) are considered and for each fluid the MMP calculation results from different methods agree well.

Chapter 2 presents the effect of heterogeneous pore size distribution on compositional distribution and recovery mechanisms. Phase compositions are altered by the effect of high capillary pressure on phase behavior, as the result, the heterogeneous pore size provides compositional gradient in reservoir domain. One example for heterogeneous pore size is the matrix-fracture interface. For such a case, there exist selective matrix-fracture mass transfer and molecular diffusion dominates the mass transportation mechanisms. Due to the selective mass transfer, fluid components redistribute between sections with different pore size and fluid properties change accordingly. Moreover, this work further investigates the change of CO_2-MMP in heterogeneous pore size reservoir when molecular diffusion is included in the model.

Chapter 3 concludes the overall work of this thesis and presents a series of key highlights from the previous two sections.

Chapter 1 Effect of Gas-Oil Capillary Pressure on Minimum Miscibility Pressure for Tight Reservoirs

Authors: Kaiyi Zhang*1; Bahareh Nojabaei1; Kaveh Ahmadi2; Russell T. Johns3
1. Virginia Polytechnic Institute and State University, 2. Pometis Technology, 3. The Pennsylvania State University

Conference paper published in the SPE Unconventional Resources Technology Conference 2018, Houston, Texas; and under review to be published in SPE journal

1. Abstract

Shale and tight reservoir rocks have pore throats on the order of nanometers, and subsequently large capillary pressure. When permeability is ultra-low (k < 200 nD), as in many shale reservoirs, diffusion may dominate over advection so that gas injection may no longer be controlled by the minimum miscibility pressure (MMP). For gas floods in tight reservoirs where k > 200 nD and capillary pressure is still large, however, advection likely dominates over diffusive transport so that the MMP once again becomes important. This paper focus on the latter case to demonstrate that capillary pressure, which impacts the fluid PVT behavior, can also alter the MMP.

The results show that the calculation of the minimum miscibility pressure (MMP) for reservoirs with nanopores are affected by gas-oil capillary pressure owing to alteration of the key tie lines in the displacement. The MMP is calculated using three methods: method of characteristics (MOC); multiple mixing cell; and slim-tube simulation. The MOC method relies on solving hyperbolic equations, so the gas-oil capillary pressure is assumed constant along all tie lines (saturation variations are not accounted for). Thus, the MOC method is not accurate away from the MMP, but becomes accurate as the MMP is approached when one of the key tie lines first intersects a critical point (where capillary pressure then becomes zero making saturation variations immaterial there). Even though capillary pressure is zero for this key tie line, its phase compositions (and hence MMP) are impacted by the alteration of all other key tie lines in composition space by the gas-oil capillary

pressure. The reason for the change in the MMP is illustrated graphically for quaternary systems, where the MMP values from all three methods agree well. The 1D simulations (typically slim-tube simulations) show agreement with these calculations as well, even though the simulations account for varying capillary pressure with saturation. We also demonstrate the impact of capillary pressure on CO_2-MMP for the real reservoir fluids. The importance of MMP for gas injection in shales as well as the effect of large gas-oil capillary pressure on the characteristics of immiscible displacements in shales and tight rocks is discussed.

2. Introduction

Unconventional oil and gas resources, such as shale gas, tight oil, and shale oil contribute significantly to hydrocarbon production in North America (Hakimelahi and Jafarpour, 2015). Although strong oil and gas demand and technological progress have led to major production increases in unconventional resources in the USA, and worldwide, in recent years, there are still significant uncertainties in understanding the complex behavior of such reservoirs as reported by Dong *et al.* (2011). Despite multiple research studies in the area, the altered phase behavior of hydrocarbon fluids in the confined space of shales and tight rocks is not yet fully understood. Numerous research studies have been conducted to investigate the phase behavior of reservoir fluids in confined space of shale reservoirs. Based on the previous studies by Zarragoicoechea *et al.* (2004) and Singh *et al.* (2009), the confined space in shale nanopores can alter the phase behavior of petroleum mixtures either by changing the petroleum mixture constituent components critical properties, such as critical pressures and temperatures, or such an alteration can be owing to large gas-oil capillary pressure in confined nanopores, which is proposed in the studies by Shapiro *et al.* (2000), Nojabaei et al. (2013), and Sugata and Piri (2015). Firincioglu *et al*. (2013) also studied the effect of Van der Waals forces on phase behavior and reported that the contribution of Van der Waals forces is small compared to capillary forces unless pores are very small (~ 1 nm)

and interfacial tension is low. Even if for fluids with very low interfacial tensions, capillary forces are 100 times larger than other surface forces when pore sizes range from 10 nm.

The studies that alter component critical pressures and temperatures will also change the critical point, which in turn can significantly impact the MMP. Teklu *et al.* (2014) pointed out that the change in the critical point significantly alters the bubble point and dew-point curves, either increasing or lowering them depending on the temperature and pressure. Whether or not the critical point should change in confined rocks is still an open research question, however.

The other end point in the literature is to assume the critical point does not vary in reservoirs with tiny pores. Nojabaei *et al.* (2013) showed that if a large capillary pressure between gas and oil is used in equilibrium flash calculations, the resulting two-phase fluid properties, including phase saturations, phase densities and viscosities, as well as dew point and bubble-point pressures can change significantly away from the critical point, similar to the results of Teklu *et al.* (2014). However, the critical point of the phase envelope does not change as interfacial tension, and hence capillary pressure, is taken to be zero there.

Hydrocarbon and non-hydrocarbon injection, such as CO_2, is an effective and common way to enhance oil recovery in conventional reservoirs. Joshi (2014) found that due to rapid production declines and low recovery factors of shale reservoirs, enhanced oil recovery (EOR) in shale oil reservoirs has attracted significant interest. Applying traditional phase behavior and simulation models to EOR operations of unconventional reservoirs, however, may fail to provide accurate results. Therefore, new algorithms are needed for reservoir simulation and phase behavior modeling based on tiny pores in such reservoirs.

Minimum miscible pressure (MMP) is a key design parameter for gas injection projects. MMP can be either measured through experiments, or calculated using numerical and analytical methods. The slim tube displacement is the most common experimental approach, first proposed by Yellig *et al.* (1980) and Holm et al (1982), to determine MMP. As for numerical and analytical methods, 1-D slim tube simulation, method of characteristics and multiple mixing cell are the three

commonly used methods in industry. Stalkup (1984) first introduced the 1-D slim tube simulation and Johns *et al* (2002) implemented this method to analysis the effect of dispersion on displacement efficiency of multicomponent oil and gas systems. Monroe *et al.* (1990) used the method of characteristics (MOC) to calculate MMP of a four-component CO_2/hydrocarbon system, and showed that there was a third key tie line in the displacement route. Johns *et al.* (1993) extended this method from four component to multicomponent mixture and pointed out that for CO_2 displacements, the key tie line controls the development of miscibility. Moreover, Johns and Orr (1996) introduced a simple geometric construction to find N_c*-3* key tie lines. Wang and Orr (1997) later rewrote the MOC problem to make it more easy to implement for real fluids. Besides these two traditional methods, Ahmadi and Johns (2011) introduced a novel multiple mixing cell method to calculate MMP. Teklu *et al.*(2012) enhanced the reliability of this algorithm by applying additional checking criterion. Later, Li *et al.* (2014) extended this method to three-phase condition. The effect of mixing and dispersion (both numerical dispersion and diffusion) on recovery, MMP and MME (minimum miscibility enrichment) was studied by Johns *et al.*, 2002, Garmeh *et al.*, 2012, and Adepoju *et al.*, 2014. They showed that mixing is scale dependent and at field scale can be quite large reducing the impact of MMP on recovery.

Similar to other fluid properties, MMP in unconventional reservoirs can be affected by nano-size confinement in shale. Zhang *et al.* (2016) accounted for a shift in critical properties in confined pores and reported that MMP could be reduced significantly for pore diameters below 50 nm. Zhang *et al.* (2017) simultaneously considered the pressure inequalities of vapor and liquid phases and the shift in fluid critical properties in their flash calculations. They reported MMP under confinement is 5.4% lower than the one with bulk fluid. Moreover, they pointed out that molecular diffusion and capillary pressure improve the oil recovery by gas injection. Zhang *et al.* (2016) showed that tie-line length is reduced by nanoscale pore confinement and therefore contributed to a lower MMP. Wang *et al.* (2016) used Perturbed-Chain Statistical Associating Fluid Theory (PCSAFT) with a parachor model to predict the CO_2 MMP for both bulk phase and nanopores, and

observed a reduction in MMP primarily caused by the shift in critical properties. Teklu *et al.* (2013) conducted a similar study and stated that there is no change of MMP due to the influence of large capillary pressure on phase equilibrium. Adel *et al.* (2018) performed CO_2 shale core flood experiments and observed that recovery factors would still increase for pressures above the MMP, and based on this observation, they concluded that MMP is not important in unconventional reservoirs. It should be noted that they measured MMPs using slim tube experiments without inclusion of nanopores confinement effect, and based on previous research, they assumed that MMP would be decreased due to confinement effect.

The motivation of the study is to examine whether MMP estimates would change for gas injection in tight rock compared to conventional reservoirs. A practical application of this research is in huff-n-puff process that has shown significant incremental oil recoveries from existing unconventional wells in shale reservoirs (Hoffman, 2018). The MMP here is defined at infinite Peclet number so that advection dominates mass transport, as governed by Darcy's law. There is still debate whether the injection into shale nanopores is dominated by advection or diffusion as there is some uncertainty on the magnitude of the Peclet number in shales. If the Peclet number is small in shales, i.e. $<< 1$ (diffusion dominated), then it is likely that the MMP defined here is not appropriate (see Cronin *et al.*, 2018). For a zero Peclet number (completely diffusion dominated) only first contact miscibility (FCM) is important. However, for tight reservoirs, and not ultra-tight ones, as long as permeability is larger than 200 nd, MMP is likely still important (Cronin *et al*., 2018).

In this paper, we calculate MMP with and without capillary pressure included in phase equilibrium calculation, using MOC, slim tube simulation and the multiple-mixing cell method. Ternary and quaternary mixtures of hydrocarbons and real reservoir fluid from the Bakken and Eagle Ford formations are considered. For the MOC and slim tube simulation, flash calculation is modified to determine MMP with capillary pressure for ternary mixtures, as well as for Bakken and Eagle Ford oil. We explain the reason for multi-contact MMP change due to large gas-oil

capillary pressure. Finally, we explore the effect of capillary pressure to further enhance the efficiency of immiscible floods.

3. Model and Methodology

MMPs for displacement of different oils by pure CO_2 are calculated and compared using three methods; slim-tube simulation, method of characteristics (MOC), and multiple mixing cells. The effect of large gas-oil capillary pressure is incorporated in the flash calculations for all three methods. The multiple-mixing cell approach with the PennPVT software (Ahmadi and Johns, 2011) is used to estimate MMPs without capillary pressure and also to examine the effect of capillary pressure on tie-line lengths for pressures below the MMP.

3.1. Assumptions

Here are the simplifying assumptions we made in our calculations.

- For MMP calculations, there is a single pore size and not a distribution of pore sizes. Although we would have a more accurate estimate of recoveries if we included pore size distribution (PSD) and saturation-dependent capillary pressure effects in the calculations (Nojabaei *et al.*, 2016), we show that the effect of PSD on the bend in the recovery curve is minimal.
- Neither gas nor oil phase pressure is changing along the slim tube. If the interfacial tension changes are minimal, it is reasonable to make these assumptions as long as we only use one pore size and not a distribution of pore sizes in the MOC and mixing cell methods.
- Mass transfer is not diffusion-dominated and Darcy's law applies. This assumption is valid for permeabilities above 200 nd (Cronin *et al*., 2018). Middle Bakken satisfies this condition.

3.2. Flash calculation with large gas-oil capillary pressure

The effect of large gas-oil capillary pressure is included in flash calculations using the approach in Nojabaei *et al.* (2013, 2016). That is, the following equations are satisfied for liquid/vapor equilibrium:

$$P^V = P + p_c \ , \quad p_c = \frac{2\sigma}{r} \tag{1.1}$$

$$f_i^V(T, P^V, y_1 \cdots y_{Nc}) = f_i^L(T, P, x_1 \cdots x_{Nc}) \tag{1.2}$$

The parameter i is the component number, which changes from 1 to N_c (total number of components) and σ is interfacial tension (IFT). P^V, P and p_c are respectively vapor pressure, reference pressure and capillary pressure. f_i^V and f_i^L are the value of fugacity of component i. The interfacial tension is calculated with the Macleod and Sugden correlation (Pederson, 2007, Nojabaei et al., 2013). Here we assume that the bulk density is uniform in the nanopores. This assumption is valid as the smallest pores in this study are larger than 10 nm in diameter (Jin and Firoozabadi, 2016). Ayirala and Rao (2006) showed that measured IFTs are underestimated by the Macleod and Sugden correlation. Thus, we increased the IFTs by a factor of three.

3.3. Slim Tube Simulation

Slim tube experiments are the most common way to measure MMP for multi-contact miscible (MCM) systems. Oil is displaced by injection gas in a slim tube at multiple constant pressures. The oil recovery factor is then plotted versus pressure after 1.2 pore volumes of gas is injected. The bend in the recovery curve indicates the estimated MMP. Slim tube simulation is a computational approach that mimics a slim-tube experiment. A simplified 1-D conservation of mass equation, shown in eq (3), is explicitly solved for compositions while pressure is fixed along the slim tube (Orr, 2007)

$$\frac{\partial C_i}{\partial t_D} + \frac{\partial F_i}{\partial x_D} = 0 \tag{1.3}$$

In this equation, t_D is dimensionless time, x_D is dimensionless distance and are defined as the following. In eq (4), *x* is the distance, *L* is the length of the medium or slim tube, Q_{inj} is the volume of injected CO_2, and *PV* is pore volume.

$$t_D = \frac{Q_{inj}}{PV} \quad , \quad x_D = \frac{x}{L} \tag{1.4}$$

C_i is the overall volumetric composition of component *i* , and F_i is the flux of component *i*, where,

$$C_i = \sum_{j=1}^{N_p} C_{ij} S_j \quad , \quad F_i = \sum_{j=1}^{N_p} C_{ij} f_j \tag{1.5}$$

Fractional flow for each phase, f_j , for a multiphase system is obtained as follows:

$$f_j = \frac{\lambda_j}{\sum_{j=1}^{N_p} \lambda_j} = \frac{k_{rj} / \mu_j}{\sum_{j=1}^{N_p} k_{rj} / \mu_j} \tag{1.6}$$

Gas and oil relative permeabilities may have different shapes in a tight system (Zhang *et al.*, 2013), however, we simply use the following correlations, as relative permeability curves do not affect the estimated MMP (where flow becomes single phase). The parameter S_{or} is the residual oil saturation and is taken to be zero here.

$$k_{ro} = (1 - S_g - S_{or})^2 \quad , \quad k_{rg} = S_g^2 \tag{1.7}$$

Oil and gas saturations, phase viscosities and densities, and *K-values* are calculated using the Peng-Robinson equation of state (Peng and Robinson, 1976). The effect of gas-oil capillary pressure is incorporated in the flash calculations and not in the flow terms, as will be explained in the discussion section.

3.4. Method of Characteristics (MOC)

The method of characteristics is a well-developed analytical method to estimate MMP. It is based on finding a set of key tie lines on the displacement path. In this paper, we use MOC to estimate MMP of quaternary mixtures with initial, injection, and crossover tie lines (Johns, 1996). MMP is the pressure at which the length of one of the key tie lines first approaches zero (i.e. the critical tie

line). A graphical illustration is used to visually investigate the effect of large gas-oil capillary pressure on the key tie line locations and MMP. Consider a mixture of component A (light), B (intermediate) and C (heavy), with an injection gas of pure CO_2. The MMP for such a system can be found by the following steps (Johns and Orr, 1996):

1. Make an initial guess and estimate the MMP at the given temperature and compositions.
2. Extend the initial tie line in the A/B/C face to zero A concentration, where A is typically the most volatile component. Record the concentration where the initial tie line intersects the zero A concentration line.
3. Find the pressure at which the critical tie line in the CO_2/B/C face also intersects the recorded concentration of step 2. This pressure is the updated MMP.
4. If the MMP from step 4 is significantly different from the one from step 1, repeat the steps to convergence.

The effect of capillary pressure is incorporated in the negative flash calculation to estimate phase compositions and the location of key tie lines.

3.5. One-dimensional fully compositional simulation

We used a 1D fully compositional simulation model to simulate CO_2 gas injection. The MRST open source code (Lie, 2016) was used and modified for this simulation. The goal is to examine the effect of variable pressures along the 1D reservoir, pore size distribution (and subsequently saturation dependent capillary pressure), and inclusion of capillary pressure in flow, on recoveries and the MMP.

4. Results and Observations

Consider first a quaternary mixture with large gas-oil capillary pressure. The multiple mixing cell method is used to estimate the MMP of a ternary mixture of C_1, C_4, and C_{10} when pure CO_2 is injected. The original oil consists of 45% C_1, 35% C_4 and 20% C_{10}. At this composition the original "oil" is initially in the two-phase region at the given temperature and pressure equal to the

calculated multi-contact MMP without capillary pressure. Penn-PVT was used to estimate the MMP of 1450 psia without capillary pressure at 160°F. Tables 1 and 2 give detail information regarding the fluid properties and binary interaction parameters used.

Table 1. Compositional data for the C1/C4/C10- CO2 system

Component	Critical Pressure (psia)	Critical Temperature (R)	Acentric Factor	Molecular Weight (lbm/lb mol)	Parachor
CO_2	1069.87	547.56	0.225	44.01	78
C_1	667.2	343.08	0.008	16.043	74.8
C_4	551.1	765.36	0.193	58.124	189.6
C_{10}	353.76	1070.831	0.5764	134	372.86

Table 2. Binary interaction parameters for the C1/C4/C10/CO2 system

	CO_2	C_1	C_4	C_{10}
CO_2	0	0.01	0.13	0
C_1	0.01	0	0.119	0.008
C_4	0.13	0.119	0	0.0847
C_{10}	0	0.008	0.0847	0

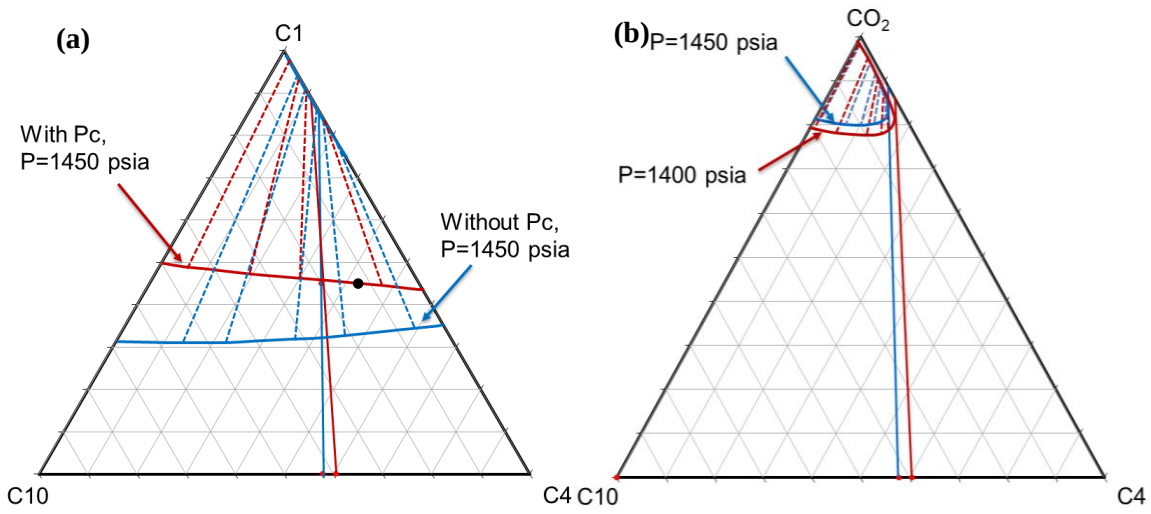

Figure 1. (a) - C1/C4/C10 binodal curves and tie lines with and without capillary, 1(b) - $CO_2/C_4/C_{10}$ binodal curves and the extension of critical tie lines at MMPs with and without capillary pressure

We used the method of characteristics, as illustrated in the methodology section, to estimate MMPs with and without capillary pressure effect. The crossover tie line is the critical tie line in this system. For the case with confinement, we considered a fixed pore radius of 5 nm. Since we already have an estimate for the MMP, we use that value as an initial guess to plot the binodal curves and the tie lines on a $C_1/C_4/C_{10}$ ternary diagram as shown in Figure 1(a). Two observations are made: first, the two-phase region with capillary pressure effect is smaller and the original oil is single phase liquid for the pressure of 1450 psia. The second observation, which we expect to influence the multi-contact MMP is that the tie lines are rotated for the case with capillary pressure. This change in the direction of tie lines, would result in two different compositions when the oil tie line intersects the C_4-C_{10} line. These two compositions would then result in two different MMPs with and without capillary pressure, as shown in Figure 1 (b). Note that the change in MMP due to capillary pressure is expected only if the crossover tie line is the critical tie line. The limiting tie line as the critical point is approached is not changed, because at the critical point capillary pressure is zero. The MMP is altered here because the oil tie line is changing. Our results show that there is approximately a 50 psi difference in the MMP of %35-%45-%20 $C_1/C_4/C_{10}$ mixture with pure CO_2 injection at 160^{o}F.The change in the direction of oil tie line gets smaller as the initial oil

composition gets closer to the original bubble-point curve. The change becomes even smaller for MMPs greater than the original oil bubble-point pressure of the original oil as the inclusion of capillary pressure does not result in a different composition when the oil tie line intersects the C_4-C_{10} line. (See Figure 2)

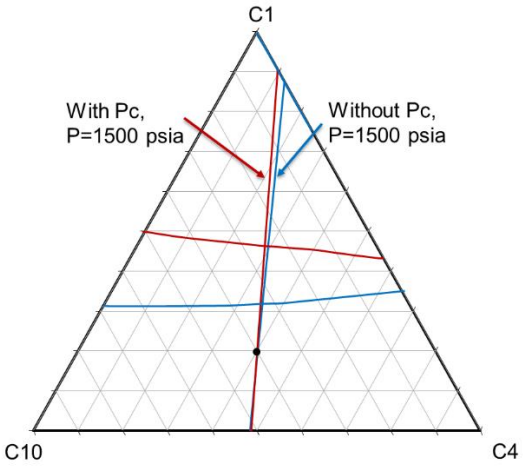

Figure 2. %20-%40-%40 C1/C4/C10 binodal curves and tie lines with and without capillary at the MMP

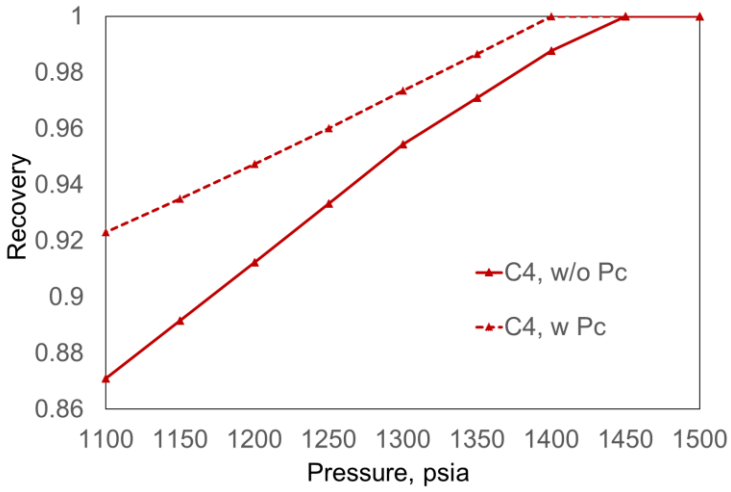

Figure 3. Intermediate component recovery as a function of pressure for cases with and without capillary pressure for the C1/C4/C10-CO_2 system

MMPs with and without capillary pressure effect are also calculated using the slim tube simulation approach. We calculated recovery of C_4, which is the intermediate component for this

case, as a function of pressure (Figure 3). The slim tube simulation results also show the same change in MMP with capillary pressure. The other indication of this plot is that recovery factor is much higher with capillary pressure at pressures well below the MMP. Recovery of C_4 is 6% higher with capillary pressure for the pressure of 1100 psia.

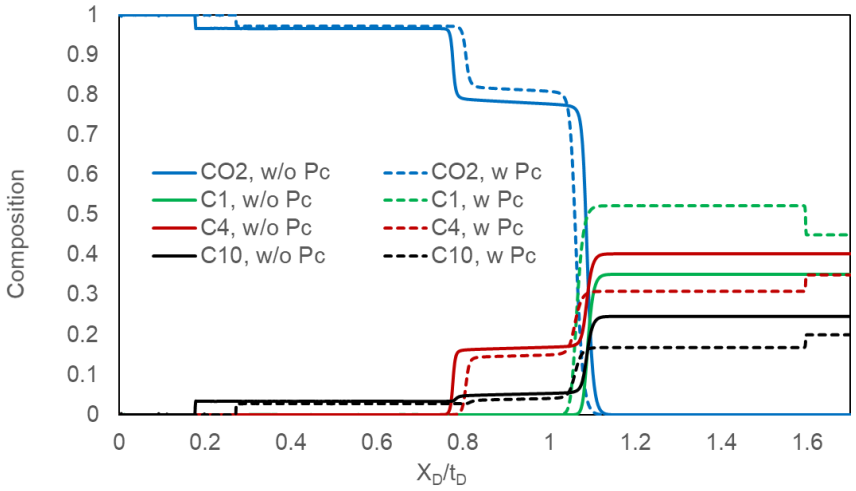

Figure 4. Composition profile as a function of dimensionless velocity with and without considering capillary pressure for the C1/C4/C10-CO_2 system

To enhance our understanding of the effect of gas-oil capillary pressure on MMPs, we made a plot of volumetric compositions along the slim tube, as a function of dimensionless velocity for the pressure of 1300 psia as shown in Figure 4. One observation is that the CO_2 front advances faster without capillary pressure effect, while the CO_2 concentration at the CO_2 front is larger with capillary pressure. Figure 5 gives the saturation fronts and shows that there is a smaller two-phase region for the case with capillary pressure, which may lead to a higher recovery.

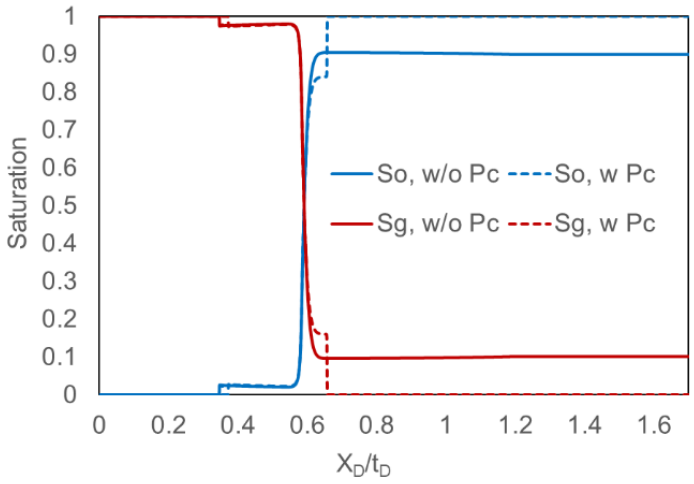

Figure 5. Saturation profile as a function of dimensionless velocity with and without capillary pressure for the C1/C4/C10-CO_2 system

The results from mixing cells method support our conclusion that MMP changes, but not significantly, when capillary pressure is accounted for in phase equilibrium calculations. For the $C_1/C_4/C_{10}$-CO_2 case, Figure 6 shows the tie line length in mixing cells after 30 contacts at 1200, 1300, and 1400 psi (slightly below the reported MMP). The contact profiles for 1400 psia for cases with pore radius of 10 nm, and without capillary pressure effects, indicate a shift on oil tie line and gas tie line but no discernible change when is at the minimum. Yet, the same 30 contacts at lower pressures (1200 and 1300 psia) show a clear difference. Tie line lengths as a function of dimensionless velocity is plotted in Figure 7, at two different pressures (one well below MMP and one right below MMP) for pore radius of 10 nm, and without capillary pressure, using slim tube simulation. The results from Figure 7 confirms that the critical tie line length is not much affected by capillary pressure when pressure is close to MMP. Figure 7 shows that capillary pressure becomes smaller and it gets to its minimum at the MMP, using the mixing cell method.

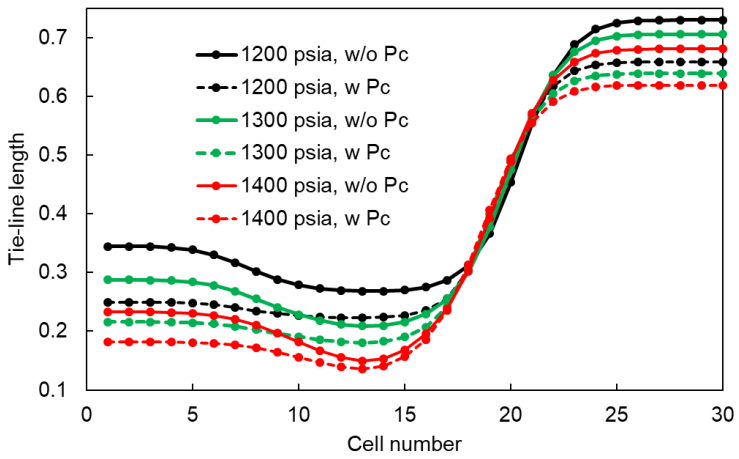

Figure 6. Mixing cells results for the effect of capillary pressure (pore radius of 10 nm) on tie line length at different pressures for the $C_1/C_4/C_{10}$-CO_2 system

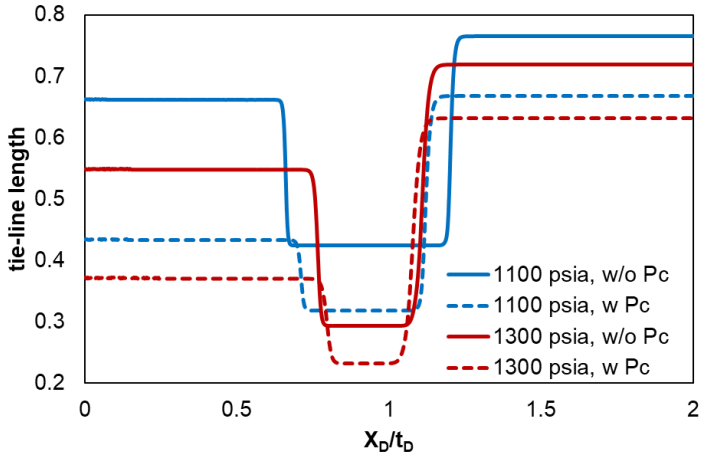

Figure 7. Slim tube simulation results for the effect of capillary pressure (pore radius of 5nm) on tie line length at different pressures for the $C_1/C_4/C_{10}$-CO_2 system

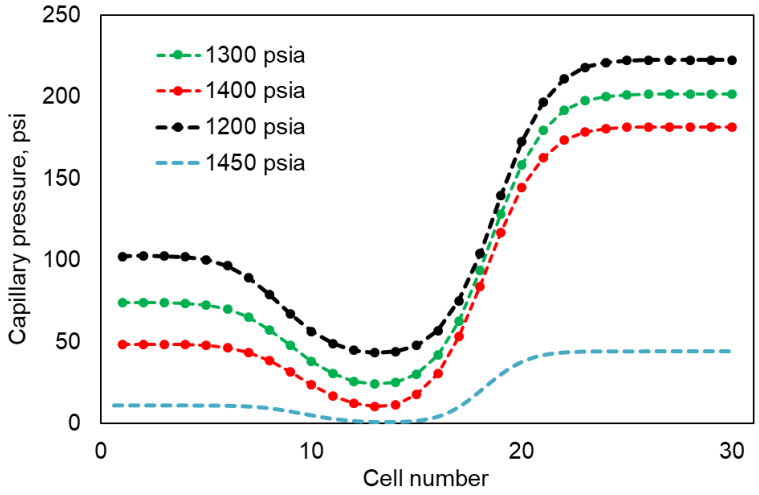

Figure 8. Calculated capillary pressures at different pressures for the $C_1/C_4/C_{10}$-CO_2 system (pore radius of 10 nm), using mixing cells method

To extend our analyses to real reservoir fluids, we used the composition of Bakken fluid as described by Nojabaei *et al.* (2013), and the pore size distribution, average pore size (modal pore throat), and permeability of a middle Bakken rock sample from Nojabaei *et al.* (2016) to run a 1D fully compositional simulation. The MMP of Bakken fluid without capillary pressure effect at reservoir temperature of 240°F, using multiple mixing cell method of PennPVT software, is 2200 psia. We considered seven various cases as for the combinations of with and without inclusion of capillary pressure in flow and flash, and also tried both a single pore size (13 nm, which is the average pore size for the Middle Bakken rock sample) and pore size distribution for the permeability of 0.01 md. For the simulation, we used 50 grid blocks, while the first and last blocks are the injector and producer respectively. The injection pressure is 200 psi higher, and the production pressure is 200 psi lower than the reservoir initial (or average) pressure. As the recovery plot of C_5-C_6 (an intermediate component for Bakken fluid) shows (Figure 9), inclusion of capillary pressure in flash results in higher recoveries at pressures well below MMP. But for pressures close to the MMP, the recovery curves for all the seven cases merge, as interfacial tension becomes small. This results verifies our previously described assumptions, as assuming no capillary pressure in flow, or using a single pore size, do not influence the MMP calculation.

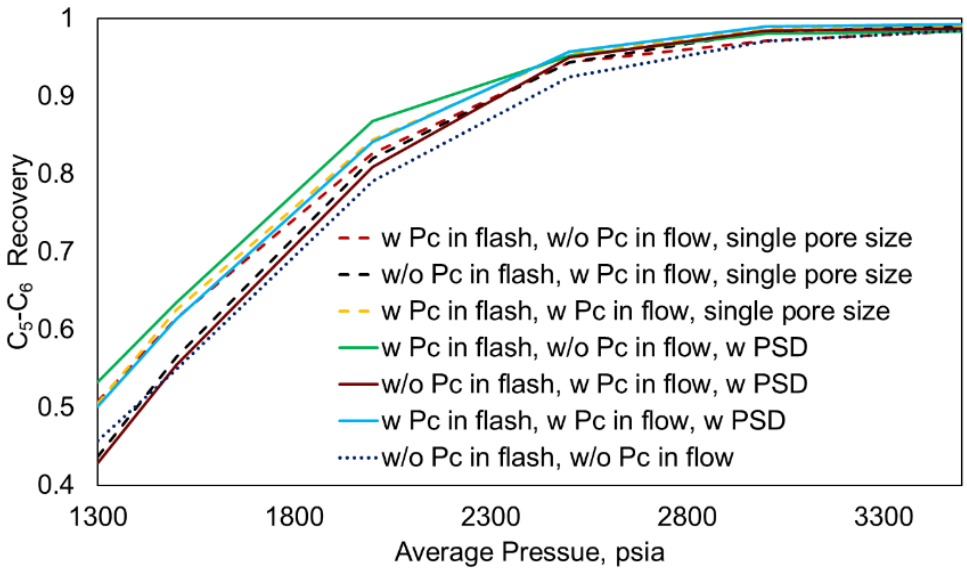

Figure 9. C5-C6 recovery as a function of pressure for displacing the Bakken fluid with CO_2, using 1D fully compositional simulation

Next, by applying slim tube simulation for a case with 10 nm pore radius, recovery-pressure plot is constructed for three pseudo-components of the Bakken fluid (shown in Figure 10). The C_5-C_6 recovery curve corresponds to approximately 2200 psia for the case without capillary pressure and this MMP result matches well with the one from multiple mixing cell. The bends in recovery curves of C_5-C_6 with and without capillary pressure effect shows that the MMP with capillary pressure is approximately 100 psi higher than that without capillary pressure. This result is in contradiction with our previous observation for the $C_1/C_4/C_{10}$ ternary mixture. To further investigate the reason why capillary pressure would increase MMP instead of decreasing it, we lumped the Bakken fluid compositions, using weight based grouping (Pedersen, 2006), down to three pseudo-components so that we can use the graphical MOC method to estimate MMPs with and without capillary pressure.

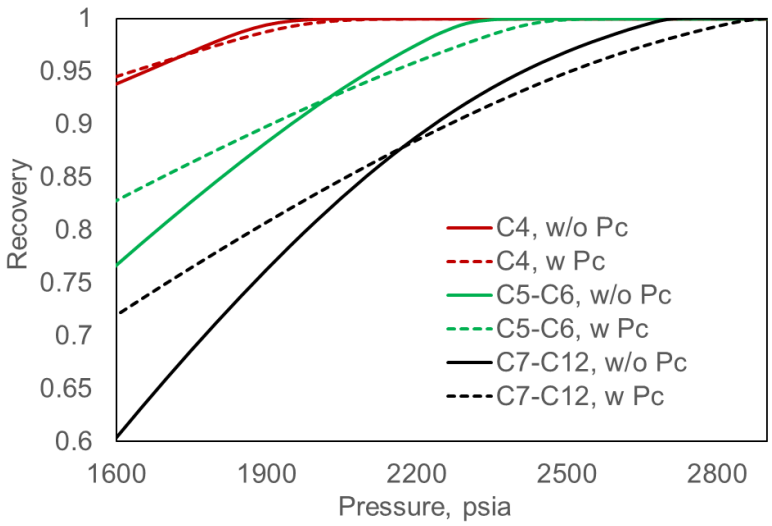

Figure 10. Components recovery as a function of pressure with and without capillary pressure for displacing the Bakken fluid with CO_2

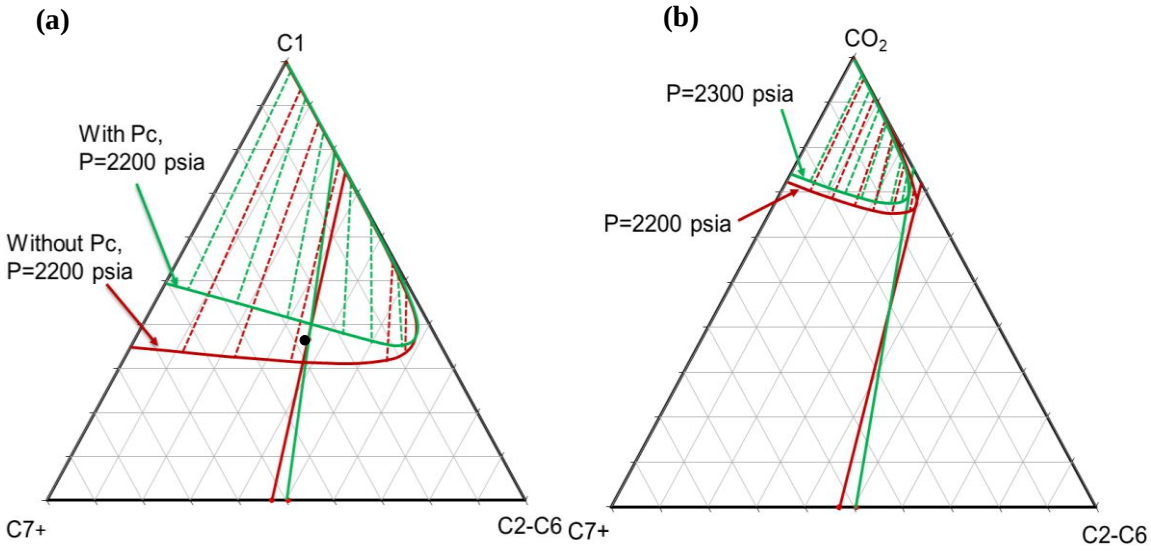

Figure 11. C1/C2-C6/C7+ binodal curves and tie lines with and without capillary, 11(b) CO_2/C_2-C_6/C_7+ binodal curves and the extension of critical tie lines at MMPs with and without capillary pressure

The binodal curves and tie lines with and without capillary pressure are plotted on the C_1/C_2-C_6/C_7+ face at 2200 psia (Bakken MMP with pure CO_2 injection without capillary pressure effect) in Figure 11(a). For this mixture, however, as shown in Figure 11(b), because of the tie lines direction in the CO_2/C_2-C_6/C_7+ face, a higher MMP is found with capillary pressure effect. Our results for the case of displacing Bakken fluid with CO_2, are consistent with the core flood

experimental results of Adel *et al.* (2018), as they also observed that further increasing pressure above the original MMP, would still result in additional recovery, which can indicate that the MMP under confinement effect might be larger than the bulk MMP.

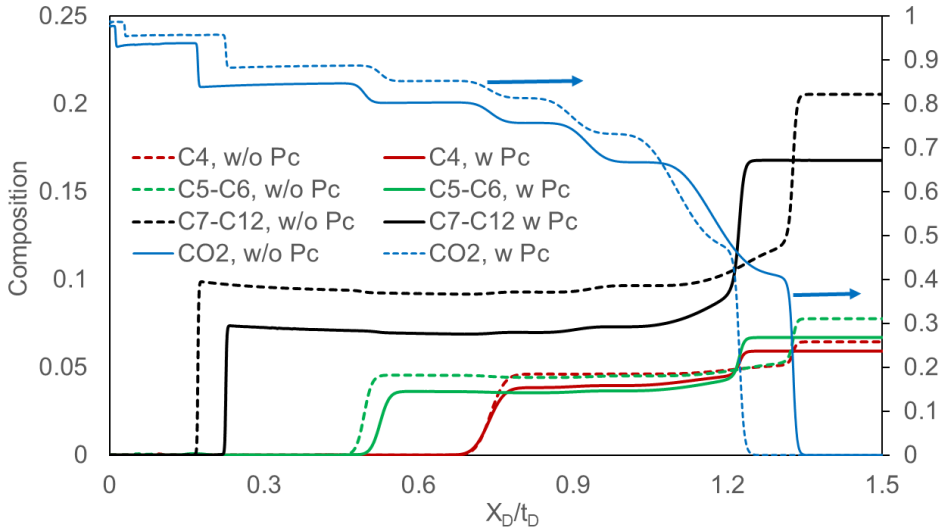

Figure 12. Composition profile as a function of dimensionless velocity with and without capillary pressure for displacing the Bakken fluid with CO_2 at 1500 psia

The composition versus dimensionless velocity is plotted at 1500 psia and it indicates that the CO_2 front is faster without capillary pressure. A faster CO_2 front can lead to a faster gas breakthrough and as a result smaller recoveries without capillary pressures at pressures well below MMP are expected, as also shown by Figure 10.

Next we analyzed the effect of large gas-oil capillary pressure on the MMP of Eagle Ford oil. We used the average pore radius of 10 nm for the capillary pressure calculations, as the pore throat diameter of Eagle Ford shale is reported to be in the range of 10-35 nm by Lewis *et al.* (2013). The Eagle Ford fluid composition and flash parameters from Siripatrachai *et al.* (2017) are used. The estimated MMP without capillary pressure by use of the multiple mixing cell method is 3200 psia. This pressure is well above the bubble point pressure of Eagle Ford fluid at the reservoir temperature of 237 ^oF. The slim tube simulation results show that the effect of gas-oil capillary pressure on MMP is minimal as shown by Figure 13. However, at pressures well below MMP, the

effect of capillary pressure is to increase recovery of the heavier components significantly. The composition change with dimensionless velocity plot of Figure 14 indicates the reason for such an enhancement in recovery, as the CO_2 front is slower and CO_2 composition at the front is higher for the case with capillary pressure when pressure is 1500 psia.

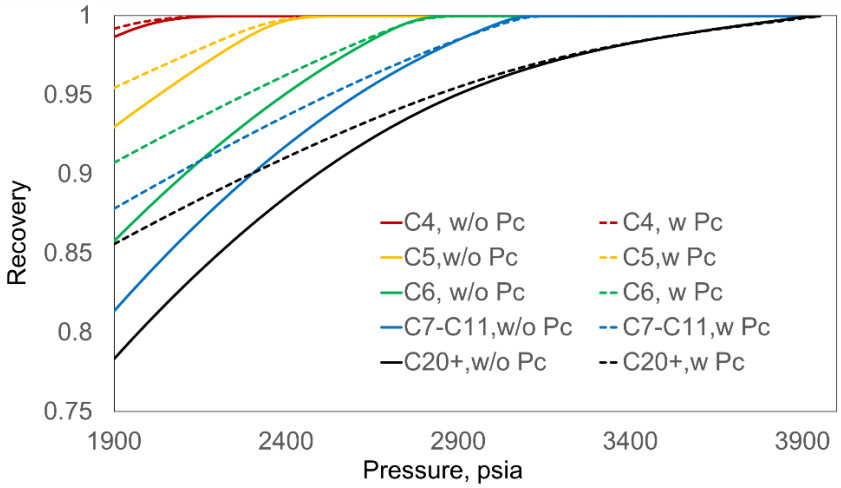

Figure 13. Components recovery as a function of pressure with and without capillary pressure for displacing the Eagle Ford fluid with CO_2

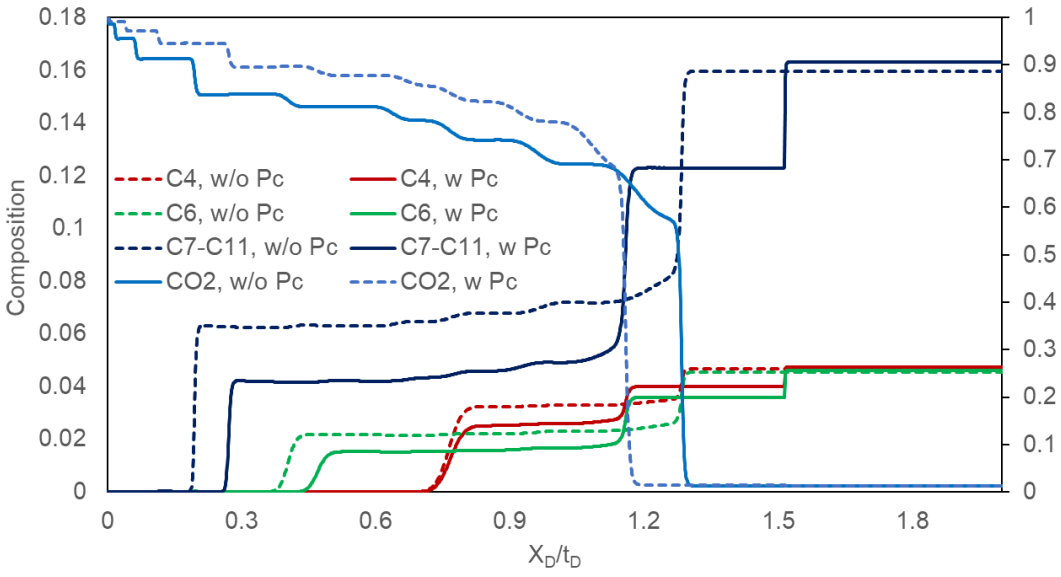

Figure 14. Composition profile as a function of dimensionless velocity with and without capillary pressure for displacing the Eagle Ford fluid with CO_2

A slower CO_2 front can imply that immiscible floods are more efficient with capillary pressure effect. It is expected that gas will break through the production well faster for the case without capillary pressure effect. These results indicate that large gas-oil pressure enhances the efficiency of immiscible gas injection in shale.

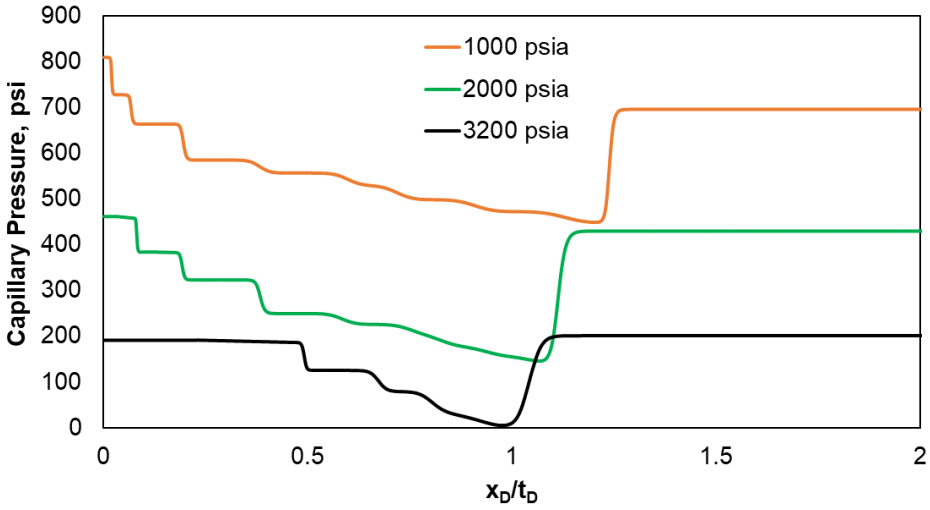

Figure 15. Capillary pressure as a function of dimensionless velocity for the case of displacing the Eagle Ford fluid with CO_2

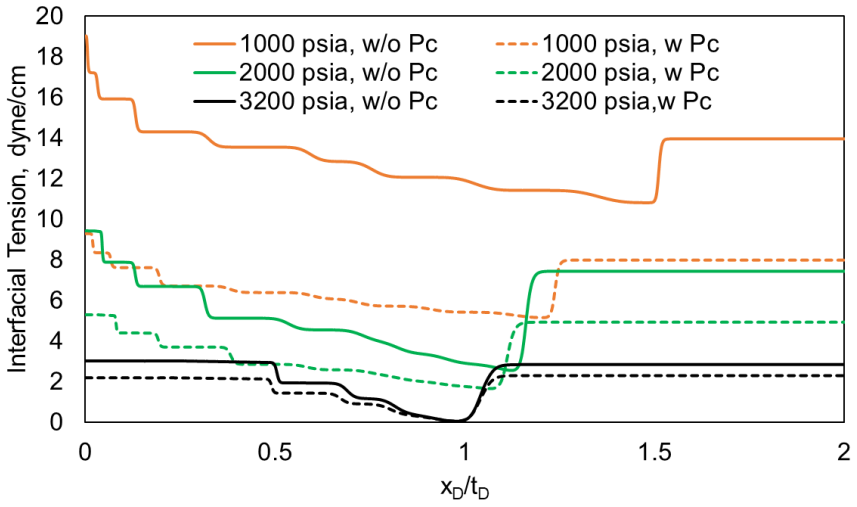

Figure 16. Interfacial tension as a function of dimensionless velocity for the case of displacing the Eagle Ford fluid with CO_2, with and without capillary pressure effect

Capillary pressure is plotted as a function of dimensionless velocity at three different pressures for Eagle Ford oil displaced by CO_2 when pore size is 10 nm (Figure 15). As this plot shows,

capillary pressure approaches zero at a certain time and location (X_D/t_D=1) at the MMP while capillary pressure in other locations on the slim tube is not zero. Interfacial tensions are also plotted for the cases of with and without capillary pressure effect in Figure 16. It can be seen that interfacial tension approaches its minimum at some point along the slim tube (zero when pressure is equal to the MMP), and the location and magnitude of this minimum at the MMP is the same with and without capillary pressure effect.

5. Discussion and Conclusions

Although it has been reported that the gas-oil capillary pressure in nanopores do not influence the MMP, our results show that capillary pressure influences MMP, however the magnitude of this change depends on the composition of the original oil, number of phases of the original oil at the MMP, and miscibility mechanisms. We confirm that the first-contact MMP is not influenced by capillary pressure as flow is single phase there.

We included the effect of large gas-oil capillary pressure for a constant pore throat size in the flash calculation of slim tube simulation, method of characteristics, and multiple mixing cells. There are certain limitations and uncertainties, such as exclusion of capillary pressure in flow or using a single pore size instead of pore size distribution and saturation-dependent capillary pressure, associated with these methods for calculating capillary pressure affected MMPs. However, we used a 1D fully compositional simulation case, to show that the complexities associated with low permeability reservoirs, do not impact the MMP calculations.

Our results suggest that the change in MMP is often negligible for practical use and often falls with 5% of the estimated MMP. One reason for this small change is that as the pressure gets close to MMP, two phases become similar (*K-values* approach unity), therefore IFT drops, and as a result, calculated capillary pressure at the equilibrium drops to a value that does not make large impact.

We also examined the effect of large gas-oil capillary pressures on the recovery efficiency of immiscible gas injection EOR and we have evidence that capillary pressure influences the effectiveness of CO_2 immiscible flood substantially for pressures well below MMP. An immiscible gas injection results in higher recoveries if the effect of capillary pressure is included in flash calculation. Note that although the MMP, which is based on oil phase pressure, does not change significantly under capillary pressure effect, the injection pressure, should be higher than the gas phase pressure in the matrix so that the required pressure gradient is provided for the gas to flow to formation.

6. Highlights

The key highlights of this research are:

- Gas-oil capillary pressure in nanopores affects multi-contact MMP of the original oil mixture with 3 components and more.
- Gas-oil capillary pressure does not affect the CO_2 MMP of a binary mixture as the only MMP is first contact.
- The effect of capillary pressure is larger if the MMP is below the original bubble-point pressure of the original oil.
- The change in MMP due to gas-oil capillary pressure does not go beyond couple of hundreds psi for the cases we examined and the reason for that is interfacial tension and subsequently capillary pressure gets smaller as the mixture gets closer to the critical region upon achieving miscibility.
- Considering the effect of gas-oil capillary pressure is important for designing immiscible gas floods.
- The results from slim tube simulation shows that capillary pressure inclusion in flash calculation slows the CO_2 front and enhances recoveries.

7. Nomenclature

C = overall volumetric composition

F = overall molar flux

f = fugacity (in equation 3)

f = fractional flow (in equation 7)

k = permeability

L = length of slim tube

P = pressure

Q_{inj} = cumulative gas injection

r = pore radius

S = saturation

t_D = dimensionless time

T = temperature

N_c = number of components

N_p = number of components

x_D = dimensionless distance

x = liquid phase molar composition

y = gas phase molar composition

z = overall molar composition

X = parachor

ρ = density

σ = interfacial tension

μ = viscosity

λ = mobility

Superscripts

L = liquid phase

V = vapor phase

Subscripts

i= component identification

j = phase identification

n = number of carbon atoms

o = oil

g = gas

8. Acknowledgements

The author would like to thank the significant contribution of Dr. Nojabaei. She conceived the idea of this paper and provided the results of method of characteristics. The author also would like to acknowledge the contribution of Dr. Johns and Dr. Ahmadi who provided the data from multiple mixing cells method and precious comments on this paper.

References

Adel, I. A., Tovar, F. D., Zhang, F., & Schechter, D. S. (2018). The Impact of MMP on Recovery Factor During CO2 – EOR in Unconventional Liquid Reservoirs, presented at SPE Annual Technical Conference and Exhibition, Dallas, Texas, USA. doi:10.2118/191752-MS

Adepoju, O. O., Lake, L. W., & Johns, R. T. (2015). Anisotropic Dispersion and Upscaling for Miscible Displacement. SPE Journal, vol. 20, no. 03, pp. 421–432.

Ahmadi, K., & Johns, R. T. (2011). Multiple-Mixing-Cell Method for MMP Calculations. SPE Journal, vol. 16, no. 04, pp. 733–742.

Ahmadi, K., Johns, R. T., Mogensen, K., & Noman, R. (2011). Limitations of Current Method-of-Characteristics (MOC) Methods Using Shock-Jump Approximations to Predict MMPs for

Complex Gas/Oil Displacements. SPE Journal, vol. 16, no. 04, pp. 743–750. https://doi.org/10.2118/129709-PA

Ayirala, S. C., & Rao, D. N. (2006). A new mechanistic Parachor model to predict dynamic interfacial tension and miscibility in multicomponent hydrocarbon systems. Journal of Colloid and Interface Science, vol. 299, no. 1, pp. 321–331.

Christiansen, R. L., & Haines, H. K. (1987). Rapid Measurement of Minimum Miscibility Pressure with the Rising-Bubble Apparatus. SPE Reservoir Engineering, vol. 2, no. 04, pp. 523–527.

Cronin, M., Emami-Meybodi, H., & Johns, R. T. (2018). Diffusion-Dominated Proxy Model for Solvent Injection in Ultra-Tight Oil Reservoirs. SPE Improved Oil Recovery Conference. Tulsa, Oklahoma, USA.

Dong, Z., Holditch, S. A., McVay, D., & Ayers, W. B. (2011). Global Unconventional Gas Resource Assessments. Canadian Unconventional Resources Conference. Calgary, Alberta, Canada.

Elahi, S. H., & Jafarpour, B. (2015). Characterization of Fracture Length and Conductivity from Tracer Test and Production Data with Ensemble Kalman Filter. Unconventional Resources Technology Conference. San Antonio, Texas, USA.

Garmeh, G., Johns, R. T., & Lake, L. W. (2009). Pore-Scale Simulation of Dispersion in Porous Media. SPE Journal, vol. 14, no. 04, pp. 559–567.

Hoffman, B. T. (2018). Huff-N-Puff Gas Injection Pilot Projects in the Eagle Ford. SPE Canada Unconventional Resources Conference. Calgary, Alberta, Canada.

Holm, L. W., & Josendal, V. A. (1982). Effect of Oil Composition on Miscible-Type Displacement by Carbon Dioxide. Society of Petroleum Engineers Journal, vol. 22, no. 01, pp. 87–98.

Jin, Z., Firoozabadi, A. (2016) Phase Behavior and Flow in Shale Nanopores from Molecular Simulations, Fluid Phase Equilibria, vol. 430, 156-168.

Johns, R. T., Dindoruk, B., & Orr Jr., F. M. (1993). Analytical Theory of Combined Condensing/Vaporizing Gas Drives. SPE Advanced Technology Series, vol. 1, no. 02, pp. 7–16.

Johns, R. T., & Orr Jr., F. M. (1996). Miscible Gas Displacement of Multicomponent Oils. SPE Journal, vol. 1, no. 01, pp. 39–50.

Johns, R. T., Sah, P., & Solano, R. (2002). Effect of Dispersion on Local Displacement Efficiency for Multicomponent Enriched-Gas Floods Above the Minimum Miscibility Enrichment. SPE Reservoir Evaluation & Engineering, vol. 5, no. 01, pp. 4–10.

Joshi, S. (2014). EOR: Next Frontier for Unconventional Oil. Journal of Petroleum Technology, vol. 66, no. 06, pp. 20–22.

Lewis, R., Singer, P., Jiang, T., Rylander, E., Sinclair, S., & Mclin, R. H. (2013). NMR T2 Distributions in the Eagle Ford Shale: Reflections on Pore Size. SPE Unconventional Resources Conference-USA. The Woodlands, Texas, USA.

Li, L., Khorsandi, S., Johns, R. T., & Ahmadi, K. (2014). Multiple Mixing Cell Method for Three-Hydrocarbon-Phase Displacements. SPE Improved Oil Recovery Symposium. Tulsa, Oklahoma, USA.

Lie, K.-A., An Introduction to Reservoir Simulation Using MATLAB: User guide for the Matlab Reservoir Simulation Toolbox (MRST). SINTEF ICT, Dec 2016.

Luks, K. D., Turek, E. A., & Baker, L. E. (1987). Calculation of Minimum Miscibility Pressure. SPE Reservoir Engineering, vol. 2, no. 04, pp. 501–506.

Monroe, W. W., Silva, M. K., Larson, L. L., & Orr Jr., F. M. (1990). Composition Paths in Four-Component Systems: Effect of Dissolved Methane on 1D CO_2 Flood Performance. SPE Reservoir Engineering, vol. 5, no. 03, pp. 423–432.

Nojabaei, B., Siripatrachai, N., Johns, R. T., & Ertekin, T. (2016). Effect of large gas-oil capillary pressure on production: A compositionally-extended black oil formulation. Journal of Petroleum Science and Engineering, vol. 147, pp. 317–329.

Nojabaei, B., Siripatrachai, N., Johns, R. T., & Ertekin, T. (2014). Effect of Saturation Dependent Capillary Pressure on Production in Tight Rocks and Shales: A Compositionally-Extended Black Oil Formulation. SPE Eastern Regional Meeting. Charleston, WV, USA.

Nojabaei, B., Johns, R. T., & Chu, L. (2013). Effect of Capillary Pressure on Phase Behavior in Tight Rocks and Shales, SPEREE, vol. 16, no. 3, pp. 281-289.

Orr, F.M., Theory of gas injection processes 2007, Tie-Line Publications.

Pedersen, K. S., Christensen, P. L., Shaikh, J. A., & Christensen, P. L. (2006). Phase behavior of petroleum reservoir fluids. CRC press.

Peng, D.-Y., & Robinson, D. B. (1976). A new two-constant equation of state. Industrial & Engineering Chemistry Fundamentals, vol. 15, no. 1, pp. 59–64.

Shapiro, A. A., Potsch, K., Kristensen, J. G., & Stenby, E. H. (2000). Effect of Low Permeable Porous Media on Behavior of Gas Condensates. SPE European Petroleum Conference. Paris, France.

Singh, S. K., Sinha, A., Deo, G., & Singh, J. K. (2009). Vapor− liquid phase coexistence, critical properties, and surface tension of confined alkanes. The Journal of Physical Chemistry C, vol. 113, no. 17, pp. 7170–7180.

Stalkup Jr., F. I. (1984). Miscible Displacement, Monograph vol.8, H.L. Society of Petroleum Engineers, 1984.

Tan, S. P., & Piri, M. (2015). Equation-of-state modeling of confined-fluid phase equilibria in nanopores. Fluid Phase Equilibria, vol. 393, pp. 48–63.

Teklu, T. W., Alharthy, N., Kazemi, H., Yin, X., Graves, R. M., & AlSumaiti, A. M. (2014). Phase Behavior and Minimum Miscibility Pressure in Nanopores. SPE Reservoir Evaluation & Engineering, vol. 17, no. 03, pp. 396–403.

Teklu, T. W., Alharthy, N., Kazemi, H., Yin, X., Graves, R. M., & Al-Sumaiti, A. M. (2013). Minimum Miscibility Pressure in Conventional and Unconventional Reservoirs. SPE/AAPG/SEG Unconventional Resources Technology Conference. Denver, Colorado, USA.

Wang, S., Ma, M., & Chen, S. (2016). Application of PC-SAFT Equation of State for CO2 Minimum Miscibility Pressure Prediction in Nanopores. SPE Improved Oil Recovery Conference. Tulsa, Oklahoma, USA.

Wang, Y., & Orr Jr, F. M. (1997). Analytical calculation of minimum miscibility pressure. Fluid Phase Equilibria, vol. 139, no. 1–2, pp. 101–124.

Yan, W., Michelsen, M. L., & Stenby, E. H. (2012). Calculation of Minimum Miscibility Pressure Using Fast Slimtube Simulation. SPE Improved Oil Recovery Symposium. Tulsa, Oklahoma, USA.

Yellig, W. F., & Metcalfe, R. S. (1980). Determination and Prediction of CO_2 Minimum Miscibility Pressures (includes associated paper 8876). Journal of Petroleum Technology, vol. 32, no. 01, pp. 160–168.

Zarragoicoechea, G. J., & Kuz, V. A. (2004). Critical shift of a confined fluid in a nanopore. Fluid Phase Equilibria, vol. 220, no. 1, pp. 7–9.

Zhang, K., Liu, Q., Wang, S., Feng, D., Wu, K., Dong, X., Dong, X., Chen, S., Chen, Z. (2016). Effects of Nanoscale Pore Confinement on CO_2 Displacement. SPE/AAPG/SEG Unconventional Resources Technology Conference. San Antonio, Texas, USA.

Zhang, K., Seetahal, S., Alexander, D., He, R., Lv, J., Wu, K., Hu, Y., Chen, Z. (2016). Correlation for CO_2 Minimum Miscibility Pressure in Tight Oil Reservoirs. SPE Trinidad and Tobago Section Energy Resources Conference. Port of Spain, Trinidad and Tobago: Society of Petroleum Engineers.

Zhang, Y., Di, Y., Yu, W., & Sepehrnoori, K. (2017). A Comprehensive Model for Investigation of CO_2-EOR with Nanopore Confinement in the Bakken Tight Oil Reservoir. SPE Annual Technical Conference and Exhibition. San Antonio, Texas, USA: Society of Petroleum Engineers.

Chapter 2 Effect of Pore Size Heterogeneity on Hydrocarbon Fluid Distribution and Transport in Nanometer-sized Porous Media

Authors: Kaiyi Zhang*[1]; Fengshuang Du[1]; Bahareh Nojabaei[1]
1. Virginia Polytechnic Institute and State University

Conference paper is accepted in the 2019 SPE Eastern Regional Meeting, Charleston, West Virginia

1. Abstract

In this paper, we investigate the effect of pore size heterogeneity on multicomponent multiphase hydrocarbon fluid composition distribution and its subsequent influence on mass transfer through shale nano-pores. Also, the change of multi-contact minimum miscibility pressure (MMP) in such environment was investigated. We use a compositional simulation model with modified flash calculation, which considers the effect of large gas-oil capillary pressure on phase behavior. We consider different average pore sizes for different segments of the computational domain and investigate the effect of the resulting heterogeneity on phase and composition distributions, and production. A two dimensional formulation is considered here for the application of matrix-fracture cross mass transfer. Note that the rock matrix can also consist of different regions with different average pore sizes. Both convection and molecular diffusion terms are included in the mass balance equations, while different reservoir fluids such as Bakken and Marcellus are considered. The simulation results show that since oil and gas phase compositions depend on the pore size, there is a concentration gradient between the two adjacent pores with different sizes. Considering that shale permeability is small, we expect the mass transfer between two sections of the reservoir/core with two distinct average pore sizes to be diffusion-dominated. This observation implies that there can be a selective matrix-fracture component mass transfer during both primary production and gas

injection EOR as a result of confinement-dependent phase behavior, which also changes the value of MMP. Therefore, molecular diffusion term should be always included in the mass transfer equations, for both primary and gas injection EOR simulation of heterogeneous shale reservoirs.

2. Introduction

Benefited from the efficiency of hydraulic fracturing and horizon drilling, production of unconventional oil and gas has grown rapidly in the past decades, making a great contribution to hydrocarbon production in North America (Boyer 2007; King 2010). Although EOR methods increased production from unconventional resources and fulfilled the strong oil and gas demand in the USA, and worldwide, there are still unknowns in complex flow and phase behavior in tight oil reservoirs.

The tight rocks pore size is in nano-scale, typically 50 nm or even smaller (Kuila and Prasad, 2011). Due to the nano-scale radius of curvature of gas/liquid interface, gas-oil capillary pressure can be several hundreds of psi large. The comparable capillary pressure will change properties of hydrocarbon mixtures, such as phase compositions, density and viscosity (Shapiro et al., 2000, Nojabaei et al., 2013 and Sugata et al., 2015). Brusilovsky (1992) studied the effect of capillary pressure on phase behavior by counting the capillary pressure difference in the phase fugacity equations. The results showed that for hydrocarbon mixtures, the bubble-point pressure decreased and dew-point pressure increased at smaller pore size. Even though he mentioned that such curvatures were unlikely to exist in hydrocarbon reservoirs, with extensive studies of tight oil resources of recent years, such phenomenon is not rarely seen any more in the confined space. Nojabaei et al. (2013) further investigated the effect of high capillary pressure on the entire PT phase envelop for binary mixtures and the Bakken fluid. They discovered that, far from the critical point, the shape of phase envelop will change. Including the large oil-gas capillary pressure, the bubble-point pressure decrease and dew-point pressure either decreases or increases depending on

the pressure. Furthermore, they found the two phase oil and gas density and viscosity would be altered considering capillary pressure in flash calculation and this change is related to the change in phase compositions. Based on previous studies, the phase behavior of hydrocarbon fluid mixture will be deviated from the original pattern in confined space due to the shift of critical properties (Zarragoicoechea et al., 2004, Singh et al., 2009). Studies revealed that the nano-confined physical space could alter the critical pressure and temperatures as well as the phase envelope. Teklu et al. (2014) showed that including critical properties shift could significantly change the bubble-point and dew-point pressures of mixtures. However, it is still an open question whether the critical point should change in confined space, such as shale matrix. Furthermore, van der Waals force also affects phase behaviors but the contribution of van der Waals forces is smaller compared to capillary pressure (Ma et al., 2013).

In conventional reservoirs, the transportation of hydrocarbon mixture in porous media is governed by Darcy's flow. However, in ultra-tight low permeability shales, the pressure gradient and gravitational drainage are inefficient (Chordia et al., 2010, Moortgat and Firoozabadi, 2013). In such environments, molecular diffusion will play an important role in oil recovery and influence mass transportation. Numerous computational and experimental research studies have been done to study the effect of diffusion on oil and gas recovery in fractured shale reservoirs. Ghorayeb and Firoozabadi (2000) studied the fracture parameters on the fluid compositional distribution. The simulation results revealed that convection took place in high permeability fractures and the composition gradient was higher for fractures with larger width. Darvish et al. (2006) simulated CO_2 injection in a fractured reservoir and concluded that the main recovery mechanism was diffusion and the contribution of gravity drainage was very small. They also pointed out that the cross phase diffusion was important. Similarly, Hoteit and Firoozabadi (2009) also stated that cross phase diffusion should be considered and based on the theory of crossflow equilibrium, they proposed a method by assuming that gas and liquid phases were in equilibrium at the interface. Moortgat and Firoozabadi (2013) indicated the existence of numerical issue of classical Fick's

model due to the exclusive definition of compositional gradient within each phase and they had numerical errors when two neighboring grid cells contain single phase fluids. This problem often occurs with sharp-phase boundaries such as in CO_2 saturated fractures. They proposed an alternative model to evade this problem by replacing compositional gradient with chemical potential gradient as the driving force. Moreover, Cronin et al. (2019) pointed out that traditional concept of multi-contact minimum miscibility pressure (MCMMP) is based on the advection dominated transport within matrix but not diffusion dominated flow and the value of MMP will be affected by high capillary pressure in nano-size confinement in shale (Zhang et al. 2016, Wang et al. 2016, Zhang et al. 2018).

The effect of nanopore confinement on phase behavior commonly occurs in nano-size pore throat of shale matrix and will alter the composition of oil and gas compared to the bulk region. For shale reservoir with nano-pore radius, compositional gradients will form within the heterogeneous pore sizes domain or during gas injection as EOR operation, such as CO_2 injection (Du and Nojabaei, 2019). In this paper, we investigate the effect of pore size heterogeneity on composition distribution of multicomponent hydrocarbon fluids and its influence on fluid properties, such as density and viscosity. The influence of diffusion on CO_2 minimum miscibility pressure (MMP) within heterogeneous pore size reservoir will also be discussed. We used an open source and multifunction reservoir simulator (Matlab Reservoir Simulation Toolbox, MRST, 2018b) and modified the compositional model of this simulator by including the effect of large gas-oil capillary pressure on phase behavior in flash calculation and adding the diffusion term in the mass balance equations. Meanwhile, a core-scale heterogeneous model (using different average pore sizes for different segments of the computational domain) was considered and its influence on phase and composition distributions and production was investigated. Two dimensional formulation is considered here to model matrix-fracture cross mass transfer while both convection and molecular diffusion terms are included in the mass balance equations. Slim-tube simulation is applied to calculate the value of MMP with heterogeneous pore size set up. The diffusion behaviors of three types of reservoir fluids,

including a ternary mixture, Bakken and Marcellus condensate in heterogeneous reservoirs are examined.

3. Model and Methodology

The effect of heterogeneous pore-size reservoir on fluid transportation and composition distribution was investigated by using a 2-D compositional simulation model, which considers the effect of large gas-oil capillary pressure in flash calculation and diffusion in the mass transport model. Here we explain about our flash calculation model, the diffusion term inclusion, and the design of pore size heterogeneity in our calculations.

3.1. Flash calculation with large gas-oil capillary pressure

In the study by Nojabaei et al. (2016), oil pressure is the reference pressure and large gas-oil capillary pressure is added to the oil pressure to calculate the gas phase pressure. Considering that there are uncertainties about the choice of the reference pressure, we modified the phase pressures calculations to allow for a reference pressure that can be either equal to the oil (liquid) pressure, equal to the gas (vapor) pressure, or in between vapor (P^V) and liquid pressure (P^L), as shown in the following equations:

$$P^V = P_{ref} + ref \times p_c \tag{2.1}$$

$$P^L = P_{ref} - (1-ref) \times p_c \tag{2.2}$$

$$p_c = \frac{2\sigma}{r} \tag{2.3}$$

$$f_i^V(T, P^V, y_1 \cdots y_{Nc}) = f_i^L(T, P^L, x_1 \cdots x_{Nc}), i = 1 - N_C \tag{2.4}$$

where p_c is the capillary pressure, ref is the adjusting parameter for the reference pressure which is between zero and one, and σ is the oil-gas interfacial tension (IFT). The interfacial tension is calculated with the Macleod and Sugden correlation (Pederson, 2007):

$$\sigma = \left[\sum_{i}^{N_c} X_i \left(x_i \bar{\rho}^L - y_i \bar{\rho}^V \right) \right]^4 \tag{2.5}$$

where X_i is parachor of component i, x_i is molar fraction of component i in liquid phase, y_i is molar fraction of component i in vapor phase, $\bar{\rho}^L$ is mass density of liquid phase, $\bar{\rho}^V$ is mass density of vapor phase.

3.2. Molecular diffusion model

For a multicomponent fluid system, the mass conservation for each component is shown as follows

$$\frac{\delta}{\delta t}(\phi \sum_{\alpha} c_\alpha^i \rho_\alpha S_\alpha) + \nabla \cdot (\sum_{\alpha} c_\alpha^i \rho_\alpha \vec{v}_\alpha + \vec{J}_\alpha^i) = \sum_{\alpha} c_\alpha^i \rho_\alpha q_\alpha \tag{2.6}$$

where $\vec{v}_\alpha$ is the overall velocity of phase α, q_α is the source term and $\vec{J}_\alpha^i$ is the Fickian diffusion flow of phase α. In hydrocarbon mixtures, each phase contains multiple components and due to Brownian motion, these components redistribute, due to the concentration or mass fraction gradient. In this study, the classic Fickian diffusion model is used to describe the diffusion behavior:

$$\vec{J}_\alpha^i = -\rho_\alpha S_\alpha D_\alpha^i \nabla c_\alpha^i \tag{2.7}$$

where c_α^i is the mass fraction of component i in phase α, ρ_α is mass density of phase α, S_α is saturation of phase α, D_α^i is the diffusion coefficient of component i in phase α. To calculate diffusion coefficients of components in oil and gas phases, Sigmund correlation (1976) as a commonly used method is applied:

$$D_\alpha^i = \frac{1-c_\alpha^i}{\sum_{i\neq j}\frac{c_\alpha^i}{D_{ij}}} \tag{2.8}$$

where D_{ij} is the binary diffusion coefficient between component i and j, which is calculated by

$$D_{ij} = \frac{\partial_\alpha^0 D_{ij}^0}{\partial_\alpha}\left(0.99589 + 0.096016\partial_{\alpha r} - 0.22035\partial_{\alpha r}^2 + 0.032874\partial_{\alpha r}^3\right) \tag{2.9}$$

where ∂_α and $\partial_{\alpha r}$ are molar density and reduced molar density of phase α; $\partial_\alpha^0 D_{ij}^0$ is the zero measure limit of the product and diffusivity in phase α. These factors can be calculated through these functions:

$$\partial_\alpha^0 D_{ij}^0 = \frac{0.0018583T^{1/2}}{\sigma_{ij}^2\Omega_{ij}R}\left(\frac{1}{M_i}+\frac{1}{M_j}\right)^{1/2} \tag{2.10}$$

$$\partial_{\alpha r} = \partial_\alpha \frac{\sum_{i=1}^{n_c} c_\alpha^i v_{ci}^{5/3}}{\sum_{i=1}^{n_c} c_\alpha^i v_{ci}^{2/3}} \tag{2.11}$$

where M_i is the molar weight of component i; σ_{ij} is the collision diameter; Ω_{ij} is the collision integral of the Lennard-Jones potential, and v_{ci} is the critical volume of component i. σ_{ij} and Ω_{ij} are calculated by the following equations:

$$\sigma_{ij} = \frac{\sigma_i + \sigma_j}{2} \tag{2.12}$$

$$\sigma_i = (2.3551 - 0.087\omega_i)\left(\frac{T_{ci}}{P_{ci}}\right)^{1/3} \tag{2.13}$$

$$\varepsilon_i = k_B(0.7915 + 0.1963\omega_i)T_{ci} \tag{2.14}$$

$$\Omega_{ij} = \frac{1.06036}{T_{ij}^{0.1561}} + \frac{0.193}{\exp(0.47635T_{ij})} + \frac{1.03587}{\exp(1.52996T_{ij})} + \frac{1.7674}{\exp(3.89411T_{ij})} \tag{2.15}$$

where ω_i is acentric factor of component i, P_{ci} and T_{ci} are critical pressure and temperature of component i, ε_i is the characteristic Lennard-Jones energy (ergs), and k_B is the Boltzmann's constant.

3.3. Heterogeneous pore-size domain set up

In order to investigate the effect of heterogeneous pore size distribution on fluid properties in fractured reservoirs, we set up a 2D simulation domain with 10m length (y), and 3mm width (x) as shown in Figure.17 below.

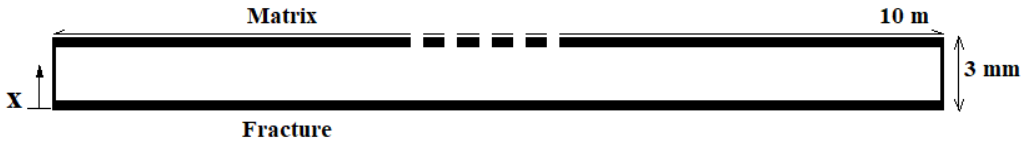

Figure 17. 2D Simulation domain setup, length of 10m and width of 3mm with pore size varying along the x direction

The pore size (r) changes along x direction, which starts from 10000nm (bulk region) to 10nm (nano-pore region) and the pore size changes with x based on the following function.

$$r \propto \frac{1}{\sin(x)} \tag{2.16}$$

The distribution of pore size and initial capillary pressure along the x direction for different fluids is shown in Figure.18.

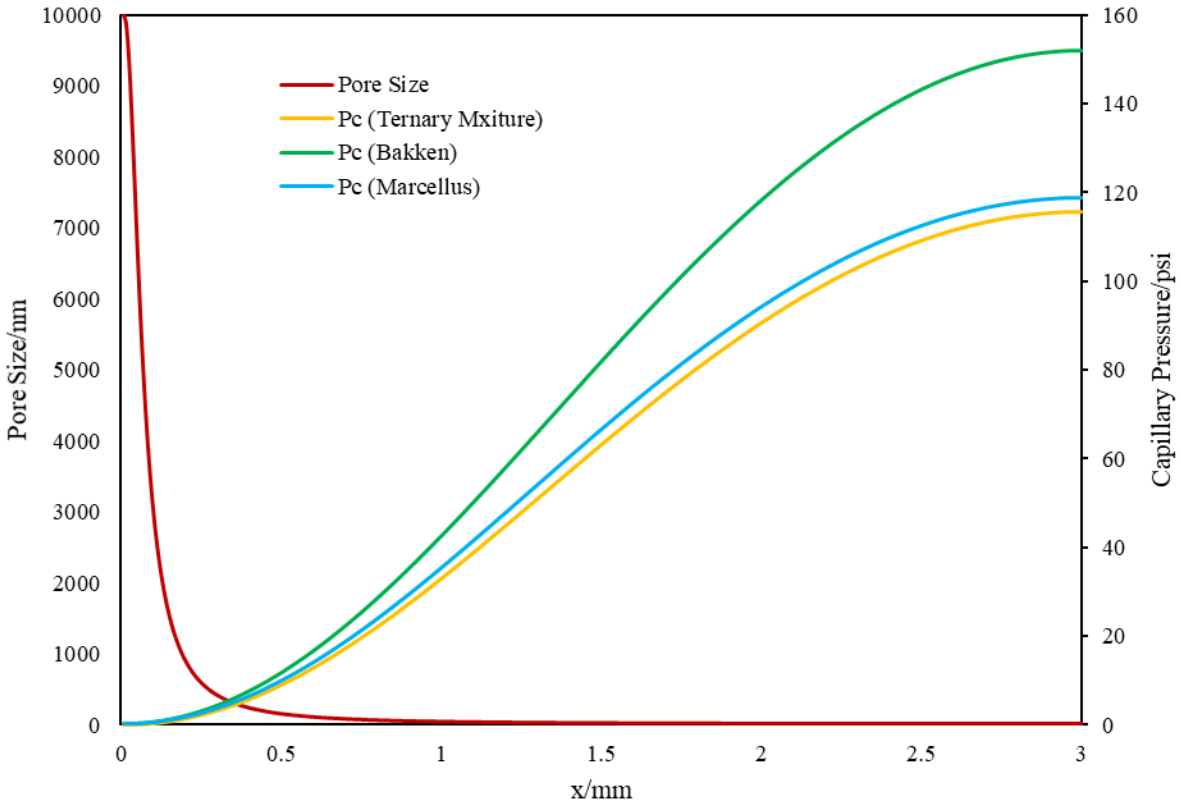

Figure 18. Pore Size and Capillary Pressure Distribution for 2-D Core-Scale Simulation Domain

3.4. Slim Tube Simulation

Multiple miscible pressure (MMP) is a key design parameter for gas injection. We used slim tube simulations to investigate the influence of molecular diffusion and heterogeneous pore size on MMP. Slim tube experiments are the most common used method to estimate multi-contact MMP. In this experiment, injection gas displaces oil in a slim tube and oil recovery factors are recorded after 1.2 pore volume of gas is injected. The oil recovery curve is plotted against pressure and the bend of this curve indicates MMP. Slim tube simulation is a numerical method to simulate the slim-tube experiment and we implemented this simulation with MRST. Here we implement heterogeneous pore size reservoir in simulation and the pore size distribution is shown in Figure 19.

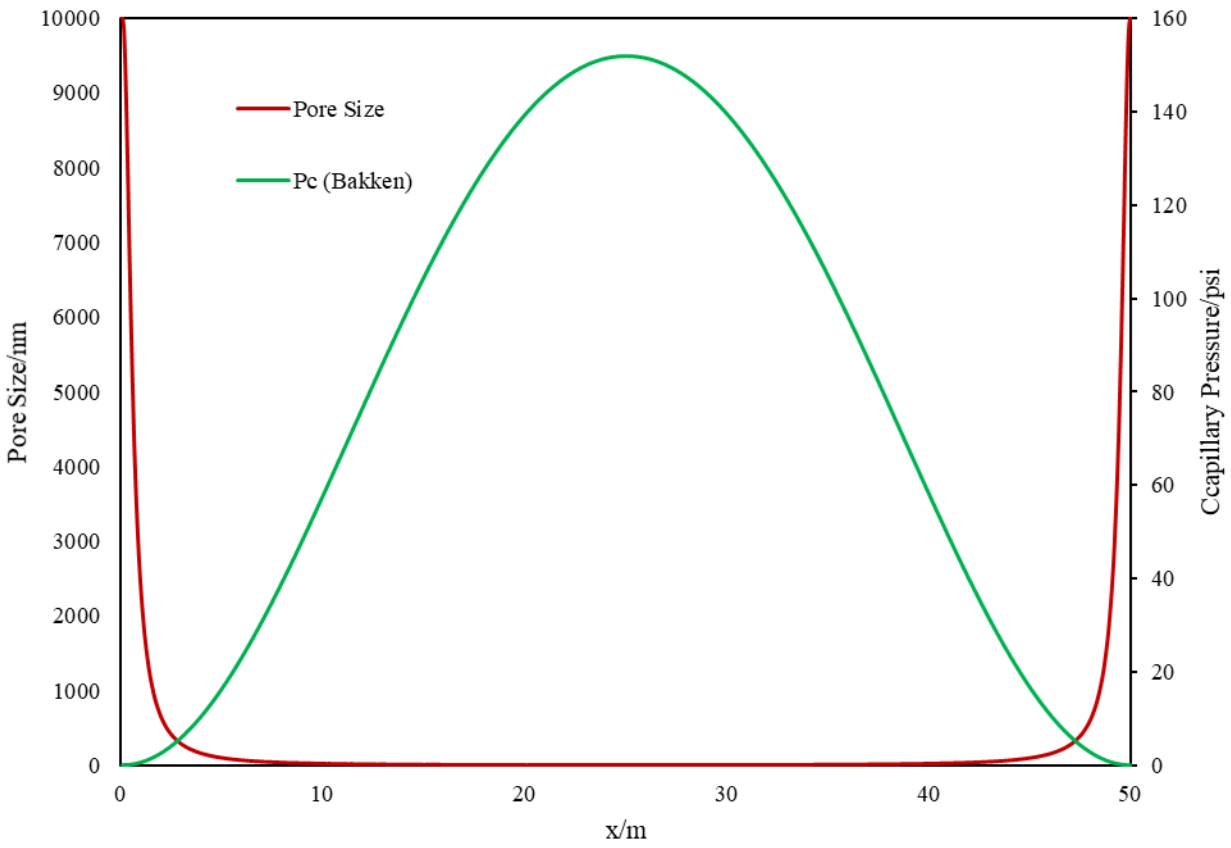

Figure 19. Pore Size and Capillary Pressure Distribution for Slim Tube Simulation

4. Results

Nanopores alter the phase behavior of multiphase multicomponent hydrocarbon mixtures, owing to the large gas-oil capillary pressure. For heterogeneous porous media, phase compositions are different in pores with different sizes, which would lead to a composition gradient. As shown in Figure 20, for a case without any source or sink term, e.g. a production or injection pressure different from the reservoir pressure, capillary pressure term in the mass balance equations provides pressure gradient for Darcy's flow and diffusion is driven by compositional gradient which is the result of the effect of inclusion of capillary pressure on phase equilibrium calculations. In this section, we first investigate the effect of molecular diffusion on the phase composition changes within a 2-D fracture-matrix setup for three different types of fluids, i.e., a simple ternary mixture, Bakken shale oil, and Marcellus shale condensate. Then, we use the ternary mixture to examine the effect of capillary pressure on viscous flow and discuss the effect of using different reference

pressures. In the last section, we combine both molecular diffusion and capillary pressure in flow and examine this combined effect on compositional profile and fluid properties.

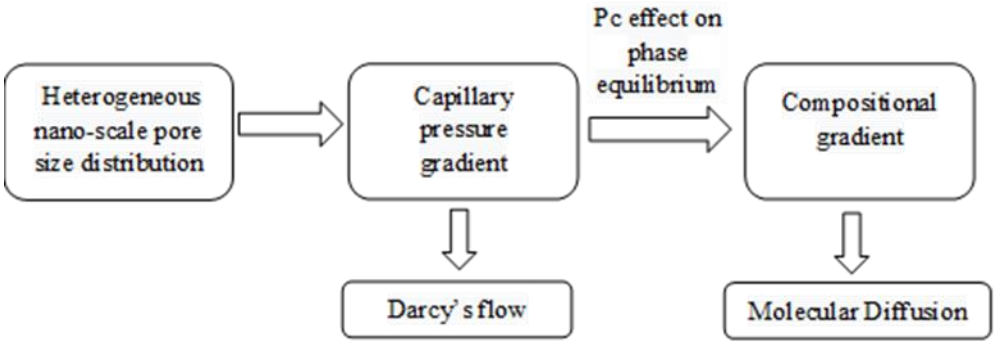

Figure 20. Effect of Heterogeneous nano-scale pore size distribution on fluid flow mechanisms

4.1. Effect of diffusion on mass transfer

To study the effect of heterogeneous pore size on molecular diffusion and its subsequent influence, we start with a ternary mixture with overall composition of 45% C_1, 35% C_4, and 20% C_{10}. The original mixture is in two phases at the given temperature of 160 °F and pressure of 1200 psia. Note that there is no pressure gradient introduced to the system. The size and properties of the 2D fracture-matrix domain is shown in Table 3. Here we set large pore sizes for the fracture and very small pores for the matrix, and we use only one value for permeability to exclude the other effects that might be connected to heterogeneous permeability. As shown in Figure 18, the pore size changes along the x direction. The fluid properties and binary interaction parameters are given in Tables 4 and 5. In the simulation model, $ref = 1$ is used to calculate phase pressure and liquid pressure is the reference pressure here. The initial phase composition is altered due to the effect of capillary pressure, as shown in Figure 21.

Table 3. Properties of the fracture-matrix 2D setup

Cell numbers	400×10
size of the system/m	0.003×10
Initial pressure/ psia	1200
Pore size/nm	As shown in Figure 18
Porosity	0.06
Permeability /nd	0.1

Table 4. Compositional data for the C1/C4/C10 system

Component	Critical Pressure (psia)	Critical Temperature (R)	Acentric Factor	Molecular Weight (lbm/lb mol)	Parachor
C_1	667.2	343.08	0.008	16.043	74.8
C_4	551.1	765.36	0.193	58.124	189.6
C_{10}	353.76	1070.831	0.5764	134	372.86

Table 5. Binary interaction parameters for the C1/C4/C10 system

	C_1	C_4	C_{10}
C_1	0	0.119	0.008
C_4	0.119	0	0.0847
C_{10}	0.008	0.0847	0

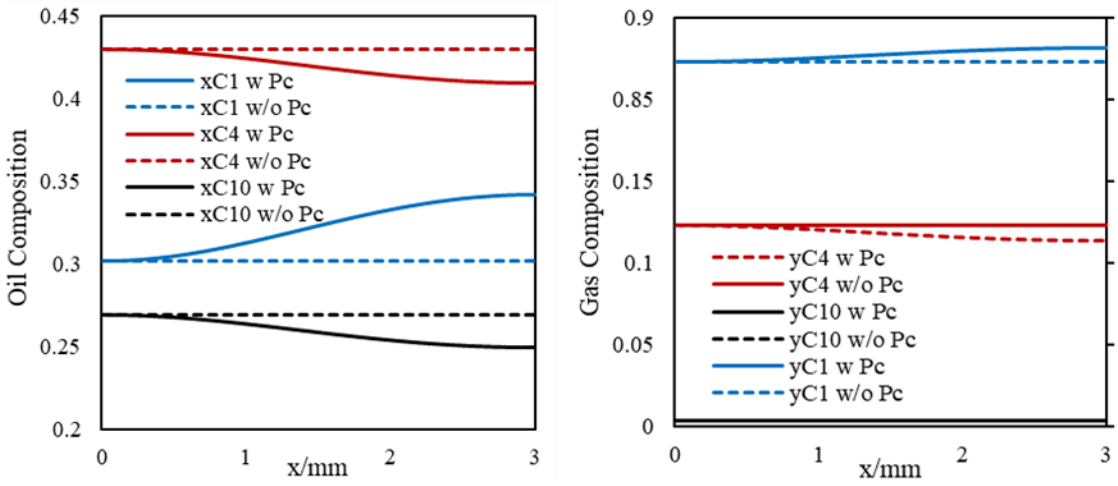

Figure 21. Initial oil and gas phase compositions with and without capillary pressure, ternary mixture

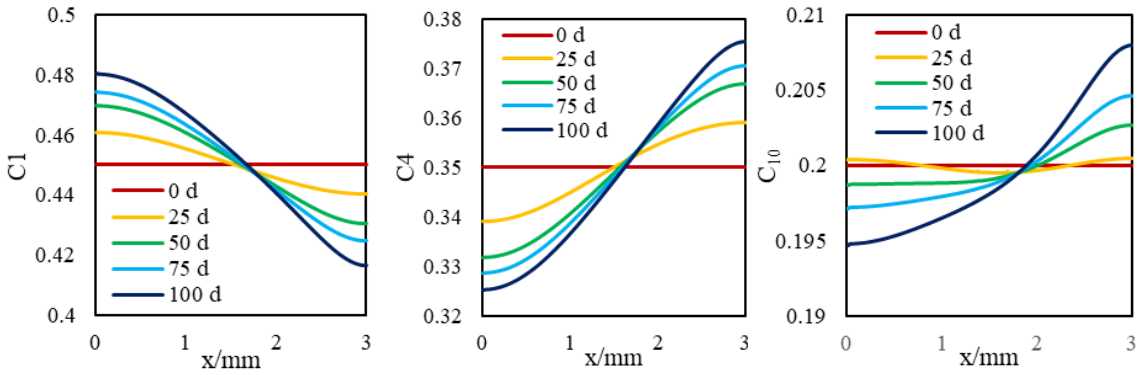

Figure 22. Overall composition of C1 (left), C4 (middle), C10 (right) at different times, ternary Mixture

It should be noted that here capillary pressure in flow is excluded and as a result, Darcy flow does not contribute to fluid transport because the pressure gradient is zero. Mass transfer is only driven by molecular diffusion caused by capillary pressure inclusion in phase behavior. Owing to the large capillary pressure in flash, the composition of each component varies at different pore radius and is changing with diffusion over time, as plotted in Figure 22. The red horizontal line represents the initial overall composition. As time goes by, the concentration of light component decreases in matrix but increases in the fracture domain and the concentration difference between the matrix and bulk region is about 6%. Intermediate components (C_4 and C_{10}) moves from the fracture domain to tight matrix and the concentration difference is about 5% and 1.5%, respectively.

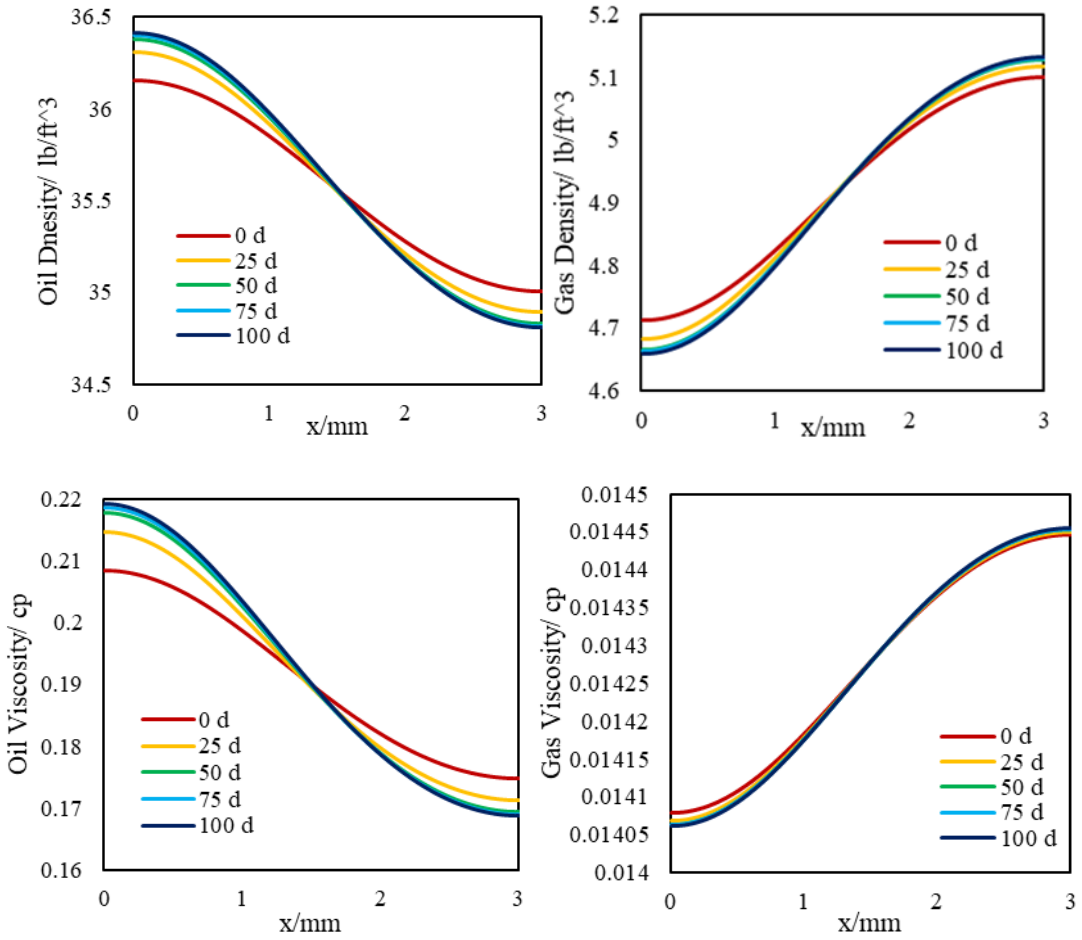

Figure 23. Oil and gas density/viscosity profile at different positions and different diffusion times, Ternary Mixture

The large oil-gas capillary pressure could not only influence the composition distribution but also alter the phase properties, such as density and viscosity. In Figure 22, the initial viscosities and densities of oil and gas vary at different location with different pore sizes. Driven by molecular diffusion, the densities of oil in fracture and gas in matrix increase while the densities of oil in matrix and gas in fracture decrease and viscosities have a similar trend. Our results show that as time passes by, the difference between oil fluid properties changes up to 50% while the difference between gas fluid properties changes around 20%.

Next, we extend our investigations to real reservoir fluids, i.e., Bakken shale oil (Nojabaei *et al.*, 2013) and Marcellus shale condensate (Elamin, 2013) while using the same simulation setup. The

reservoir temperatures of Bakken shale oil and Marcellus shale condensate are at 240°F and 150°F, respectively.

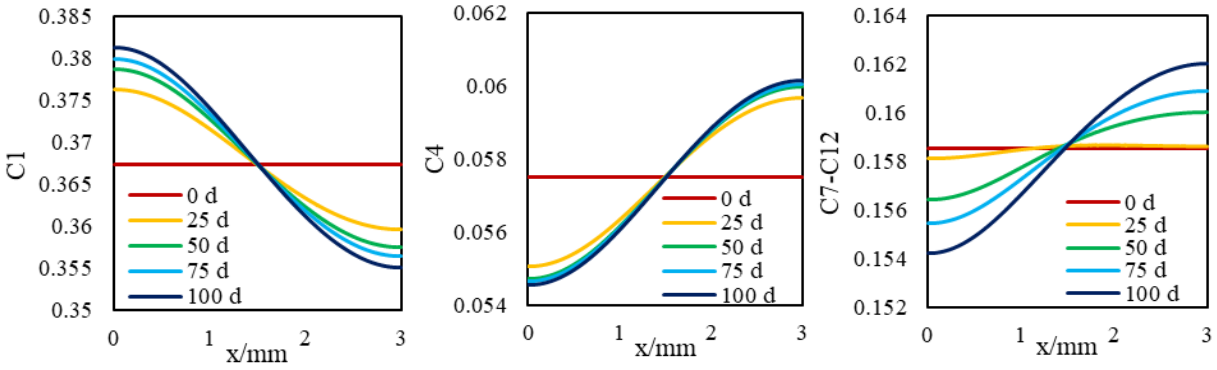

Figure 24. Overall composition of C1 (left), C4 (middle), C7-C12 (right) at different times, Bakken shale oil

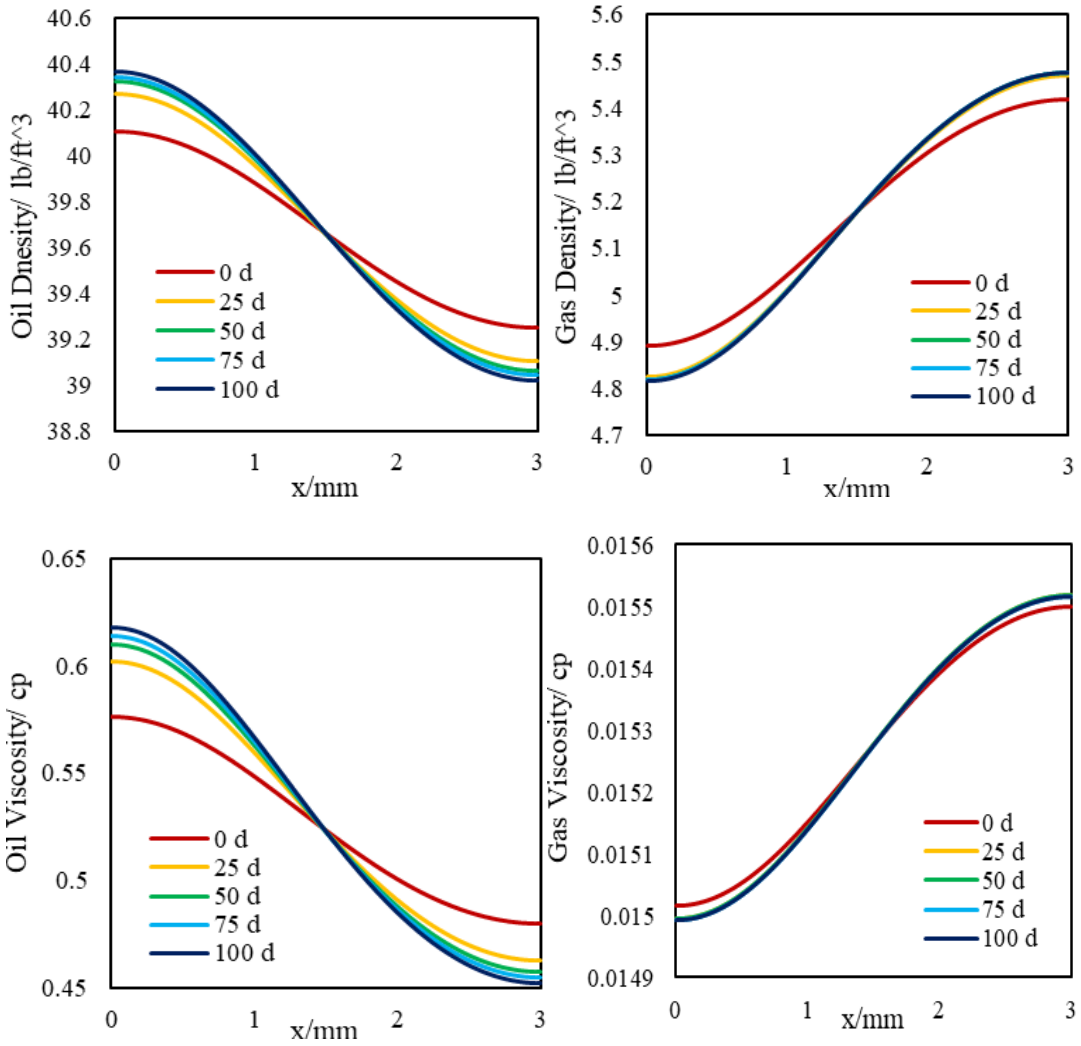

Figure 25. Oil and gas density/viscosity profile at different times, Bakken shale oil

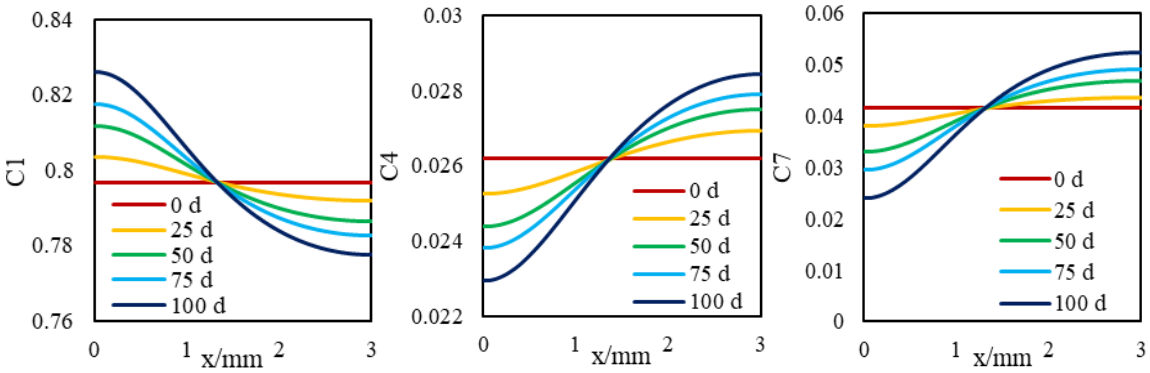

Figure 26. Overall composition of C1 (left), C4 (middle), C7 (right) at different times, Marcellus shale condensate

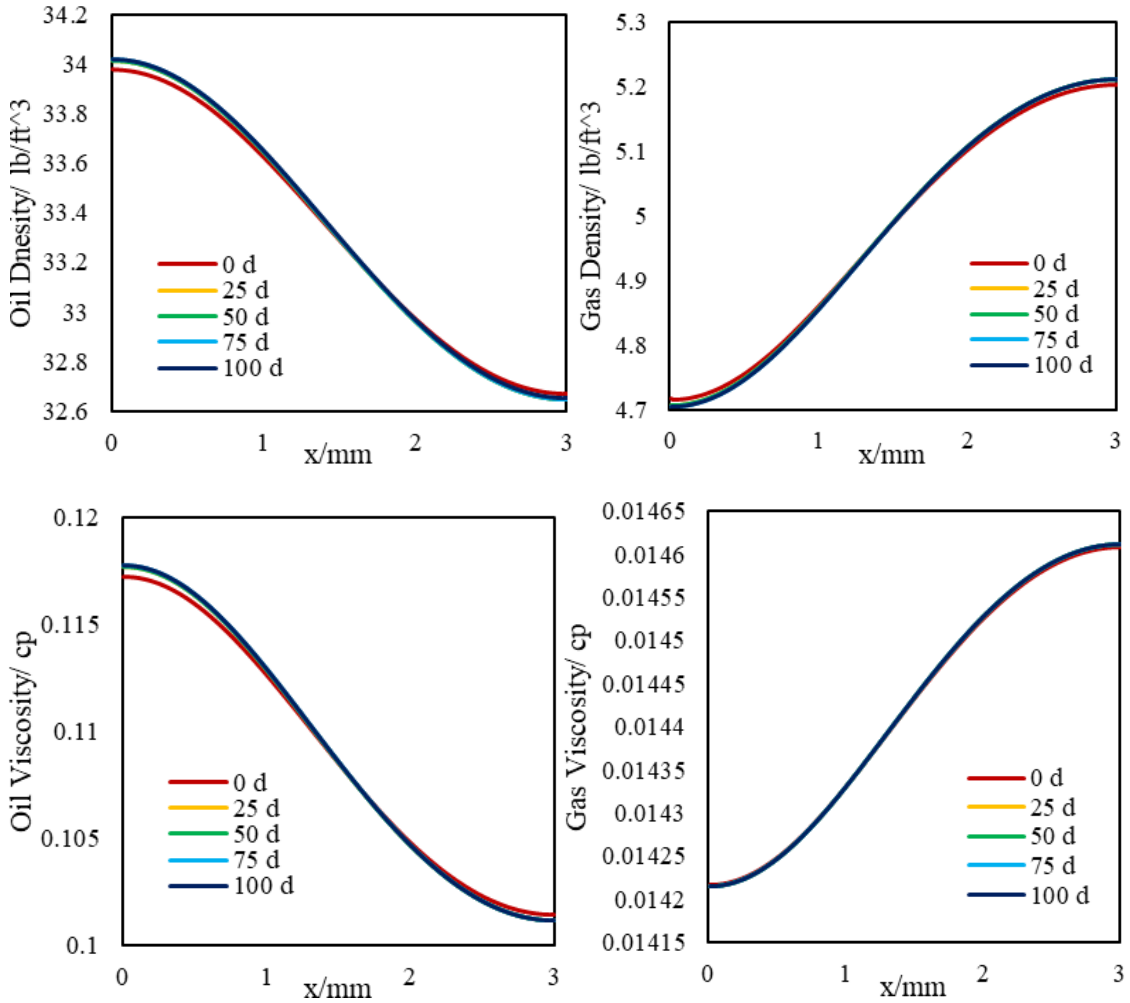

Figure 27. Oil and gas density/viscosity profile at different times, Marcellus shale condensate

The composition distribution and oil/gas viscosity and density of Bakken shale oil and Marcellus shale condensate are plotted in Figures 24-27. The results of overall composition profiles are similar

to the ones for the ternary mixture. As shown in Figure 24 and Figure 26, for both shale fluids, the composition of the light component (C_1) increases in fracture and decreases in the matrix, while the intermediate components, i.e. C_4, C_7-C_{12} (Bakken oil), and C_4, C_7 (Marcellus condensate), transfer from the fracture to matrix. The change of fluid properties for Bakken fluid is also similar to the ternary mixture. As shown in Figure 25, the densities and viscosities of oil in fracture and gas in matrix increase while the densities and viscosities of oil in matrix and gas in fracture decrease. However, for Marcellus shale condensate, the fluid proprieties are barely changed (Figure 27). This is because the methane composition is dominated (80%) over other components and the change of methane in composition (around 3%) has little effect on the fluid properties.

In summary, due to the effect of heterogeneous pore-size distribution, molecular diffusion and mass transfer occur at the fracture-matrix interface. In general, light components move from matrix region to fracture, while intermediate components migrate in the opposite direction, i.e., from fracture to matrix. We should note that the component redistribution happens for all fluids cases and the trends are similar, but the change of fluid properties varies with fluid composition. For Bakken fluid, its density and viscosity change by 3% and 5%, respectively, but for gas condensate fluid, the density and viscosity barely change with time.

4.2. Inclusion of capillary pressure in flow.

Driven by compositional gradient only, fluid overall compositions and mass changed over time because of molecular diffusion. However, capillary pressure itself acts as a driving force and influence the composition distribution. In this section, we study the effect of capillary pressure inclusion in flow on mass transfer for the ternary mixture using the same 2D simulation setup. We examine different choices of the reference pressure ($ref = 1$, $ref = 0.5$ and $ref = 0$) to analyze the effect on composition redistribution. Figure 28 shows the results of composition profiles with different reference pressure choices after 100 days. It is observed that the light component moves

toward the bulk (fracture) region and the intermediate component moves from the fracture to matrix and this trend is the same as the previous results when diffusion is considered only. The selection of different reference pressures barely change the composition distribution. Basically, as reference pressure equals to liquid (vapor) pressure, i.e. $ref = 1$ ($ref = 0$), the composition difference between both sides will reach a maximum (minimum) value and the difference between the maximum and the minimum value is around 1%.

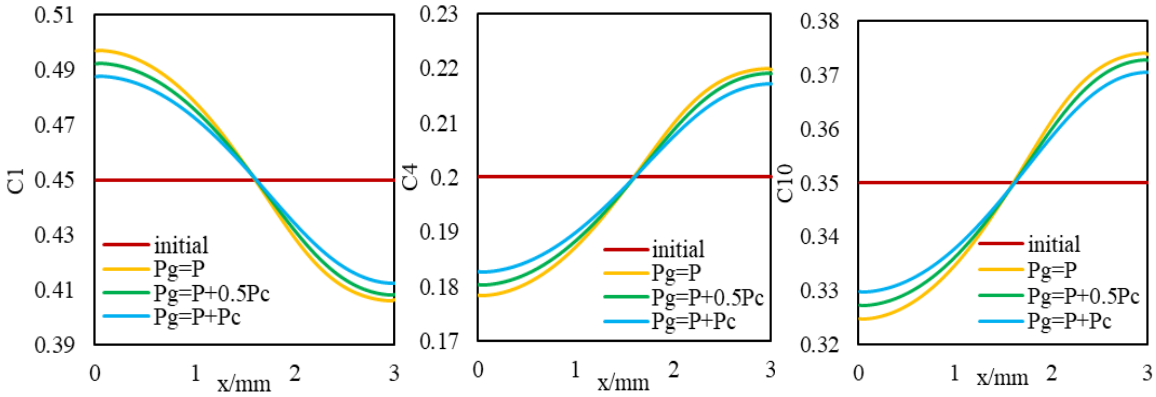

Figure 28. Overall composition of C1 (left), C4 (middle), C10 (right) with different reference pressures, Ternary Mixture, w Pc in flow/wo diffusion

Next, the oil and gas properties for different reference pressure choices are calculated. As shown in Figure 29, for any reference pressure choice, the difference between the fluid properties at the two ends (matrix and fracture) decreases with time, and this observation is the opposite of what we observed due to diffusion only. In addition, different reference pressure choices yield density and viscosity distribution.

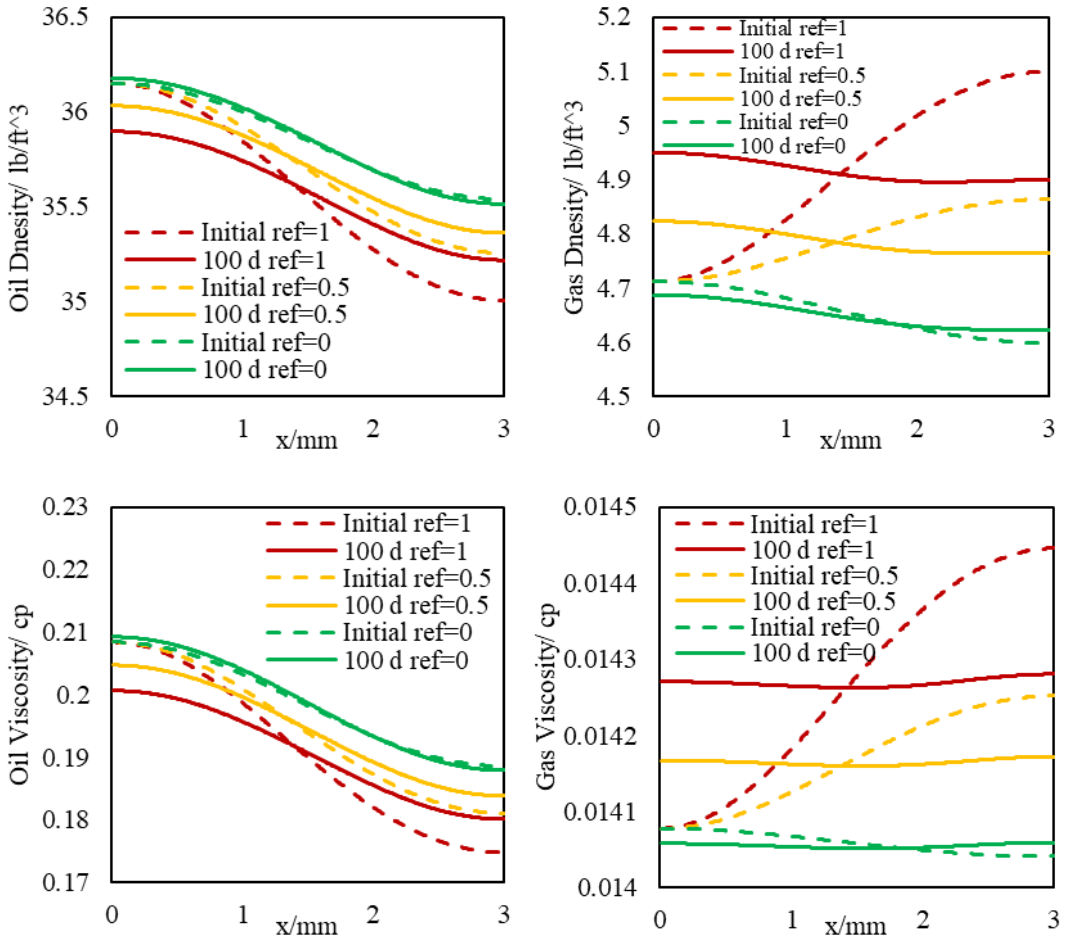

Figure 29. Oil and gas density/viscosity profile with different reference pressures, w Pc in flow, w/o diffusion, 100 days, Ternary Mixture

4.3. Diffusion and capillary pressure in flow combination effect

Finally, both molecular diffusion and capillary pressure in flow are incorporated in our simulation model. The ternary mixture fluid is used and the liquid pressure is selected as the reference pressure, i.e. *ref=1*. The results and the comparison with previous cases are shown in Figures 30 and 31. As shown in Figure 30, for the model with consideration of only diffusion or capillary pressure (Pc) in flow, light component accumulates in the bulk (fracture) region and the concentration of the intermediate component increases in the matrix nanopores. When both driving forces are considered, the trend of composition redistribution is amplified compared to either of the single effects. The fluid properties difference at the two boundaries increase in diffusion model but

decrease in the model with capillary pressure in flow only. When both molecular diffusion and capillary pressure in flow are considered, the two effects (yellow and green lines) would cancel each other out and the final fluid properties (blue lines) are close to the initial case (red lines).

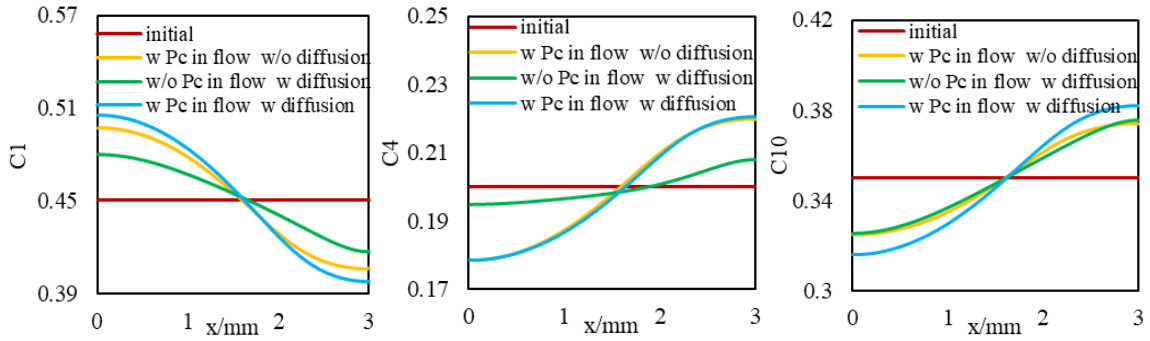

Figure 30. Overall composition profile, w Pc in flow/wo diffusion vs. wo Pc in flow/w diffusion vs. w Pc in flow/w diffusion, 100 days, Ternary Mixture

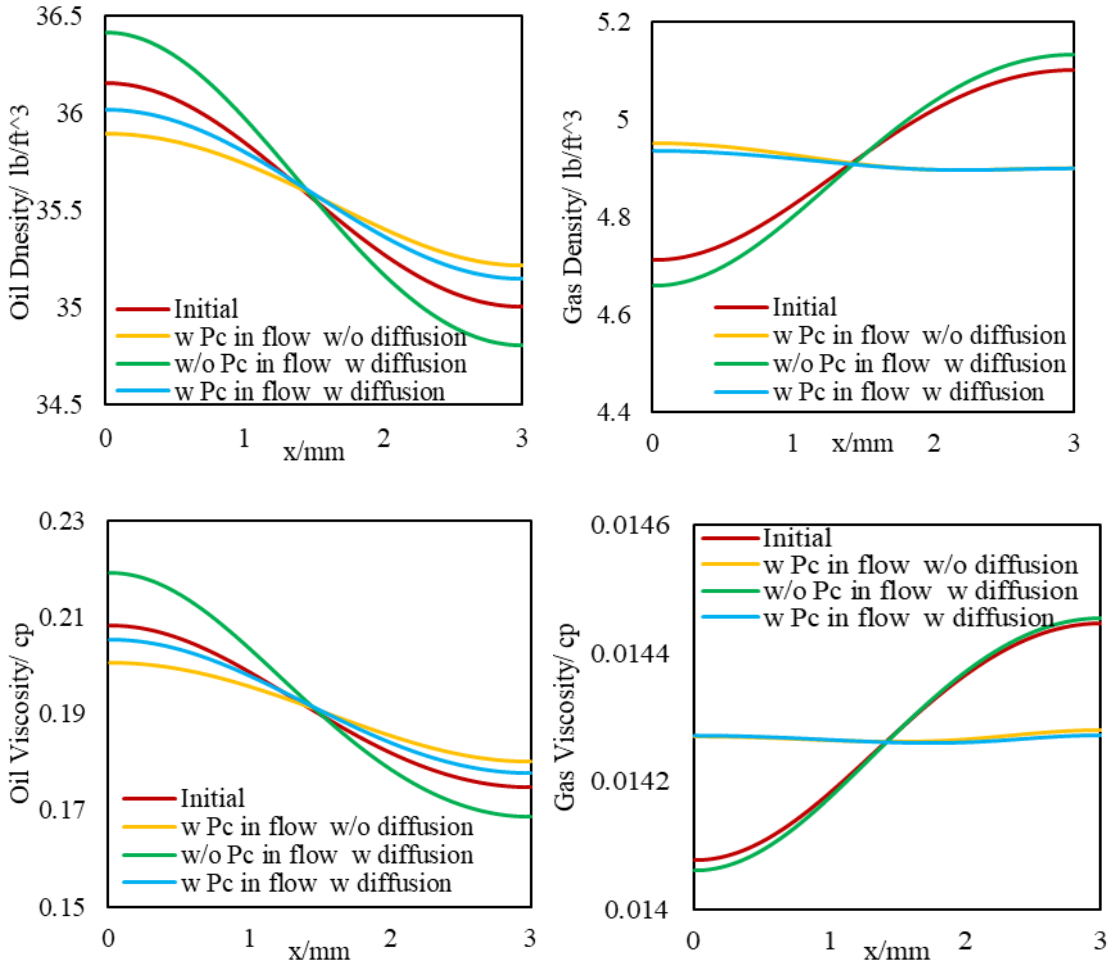

Figure 31. Oil and gas density/viscosity profile, w Pc in flow/wo diffusion vs. wo Pc in flow/w diffusion vs. w Pc in flow/w diffusion, 100 days, Ternary Mixture

4.4. Slim tube simulations

We used slim tube simulations (1-D fully compositional model) to investigate the influence of molecular diffusion and heterogeneous pore size on MMP for Bakken fluid. We set up three groups of simulations with different permeabilities, i.e. 10ud, 1ud, 100nd, the other information of slim tube simulation set up are shown in Table 6. For each group, we test different models (with and without diffusion) and different pore size distributions, i.e. homogenous 10um, heterogeneous pore size (Figure 19). Note that the effect of capillary pressure is considered both in flow mechanism and flash calculation.

Table 6. Properties of slim tube simulation setup

Cell numbers	50×1
Size of the system/m	50×1
Initial pressure/ psia	1300/1500/2000/2500/3000/3500 psi
Pore size/nm	10μm/heterogeneous (Fig.3)
Porosity	0.06
Permeability	10μd/1μd/100nd
Wells position (Injection/production)	Left end/Right end (x=0m/x=50m)

Figure 32, 33 and 34 respectively shows the recovery curves of C_5-C_6 of slim tube simulation with 10μd, 1μd and 100nd permeability. As shown in these figures, all the C_5-C_6 curves without diffusion approximately bend at the same point of pressure, 2600psi, even though pore size distributions are different. For pressures below the bending pressure, the C_5-C_6 recovery of heterogeneous pore size reservoir is lower (about 15%) than the case with homogenous 10nm pore size but higher (about 2%) than the case with homogenous 10μm pore size. For the cases with diffusion, it can be seen that the bend in the recovery curve is happening at higher pressure as

permeability is decreasing. If we extrapolate this bending pressure to permeability close to zero, we will get to the same pressure as the first contact minimum miscibility pressure (FCMMP) of CO2 and Bakken oil, which is 4940 psia from swelling test as shown in Figure 36. These results are consistent with the conclusion of Cronin et al. (2019) stating that for diffusion-dominated systems, only FCMMP is important and MCMMP is not applicable in gas flooding of ultratight reservoirs. Similarly, for pressures lower than MMP, the recovery of heterogeneous pore size reservoir is lower than homogenous 10nm pore size reservoir but higher than homogenous 10µm pore size reservoir. However, for any pressure, the recovery of the case with diffusion is lower than the case without diffusion. Furthermore, for the cases with the same pore size set up, the recovery difference between with and without diffusion increases with decreasing of reservoir permeability. The average difference for each case is, 12% (10µd), 20% (1µd) and 30% (100nd)

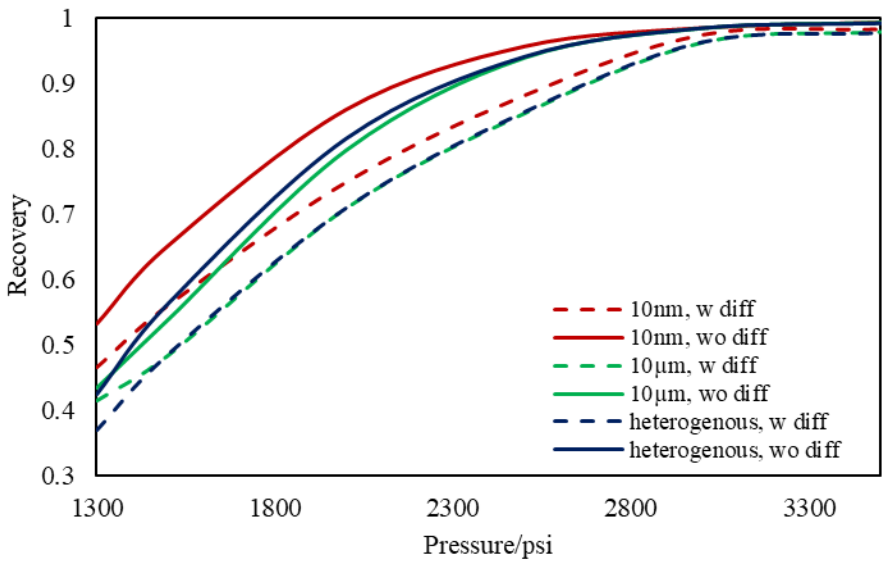

Figure 32. C_5-C_6 Composition recovery as function of pressure with and without diffusion for slim tube simulation, Bakken, 10µd

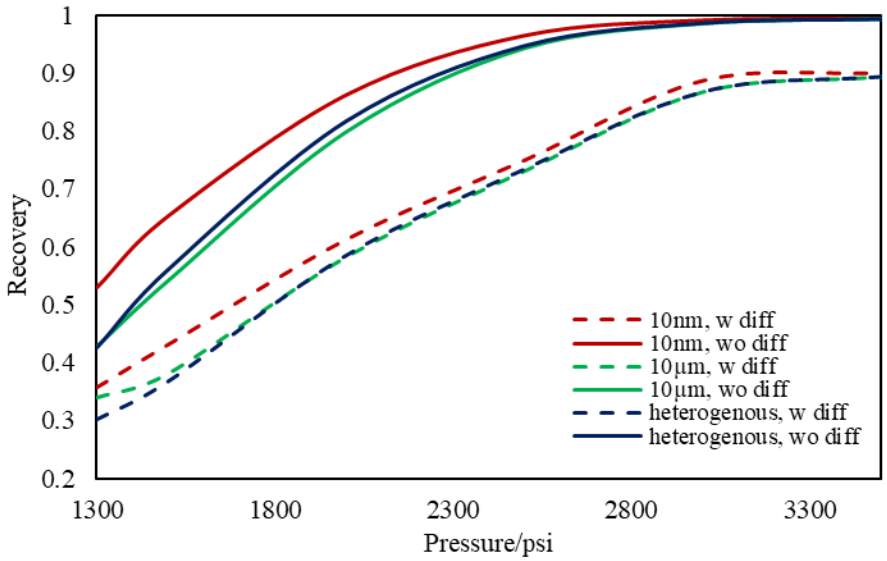

Figure 33. C_5-C_6 Composition recovery as function of pressure with and without diffusion for slim tube simulation, Bakken, 1µd

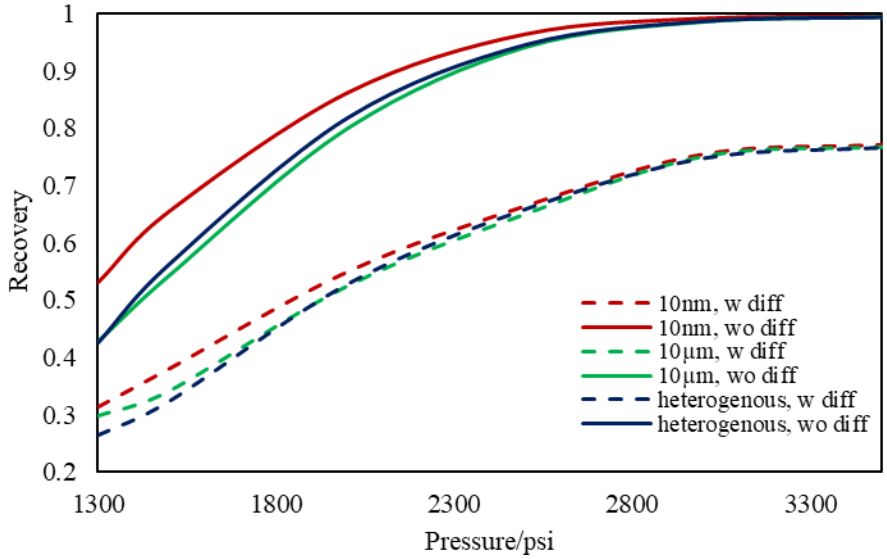

Figure 34. C_5-C_6 Composition recovery as function of pressure with and without diffusion for slim tube simulation, Bakken, 100nd

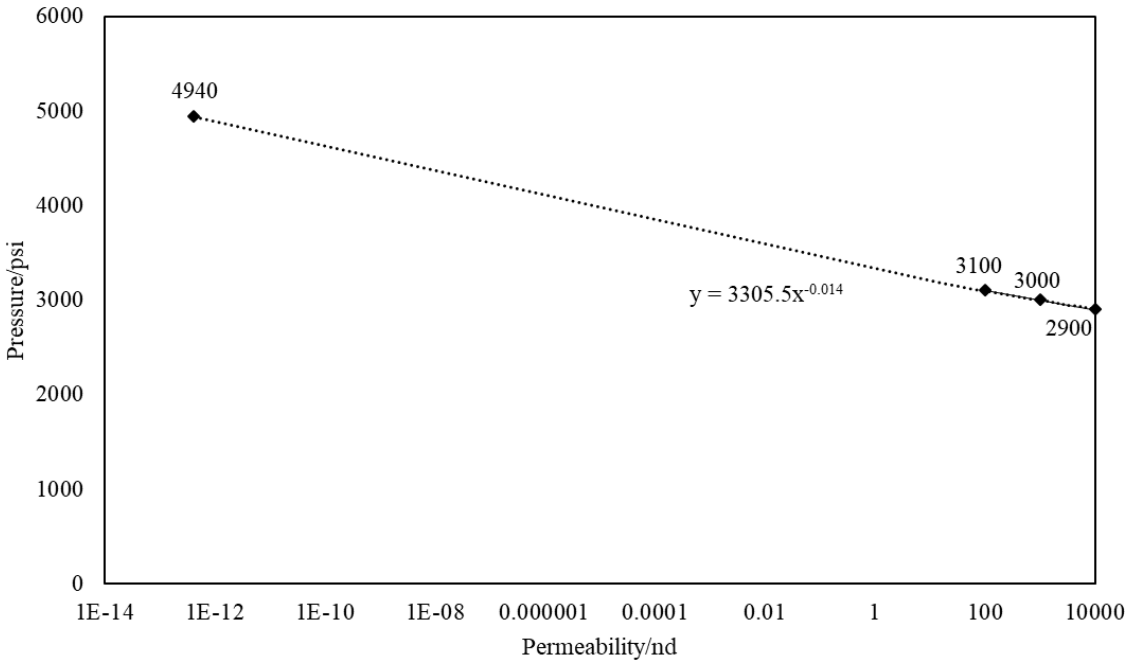

Figure 35. Recovery bending pressures of slim tube simulation vs. permeability with diffusion, Bakken

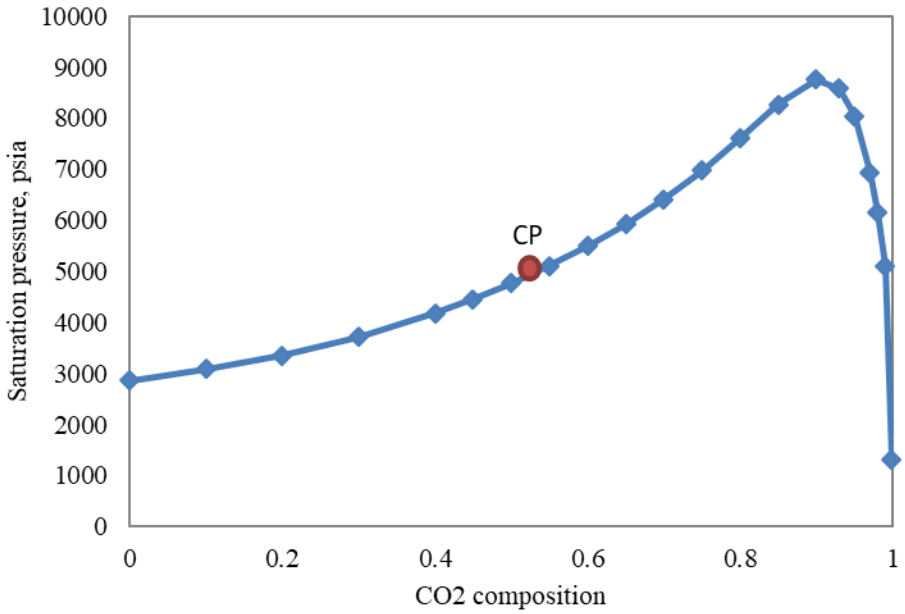

Figure 36. Swelling test for Bakken-CO_2 fluid

5. Discussion and Conclusion

The results showed that the heterogeneous pore size distribution in reservoir, such as natural fractures in the matrix, influences the distribution of fluid composition. The light components accumulate in the bulk region (or fracture) and the heavier components accumulate in the nano-pore region (shale matrix). Meanwhile, the fluid properties also vary in these regions. Molecular

diffusion and the pressure gradient capillary pressure gradient driven convection are the two important mechanisms for fluid transport.

Diffusion cannot exist without phase composition gradient and it only occurs for oil-gas two phase systems. Note that diffusion tends to decrease this phase composition gradient over time until an equilibrium is reached. In our study, heterogeneous capillary pressure enlarges concentration gradient due to its effect on phase equilibrium. If capillary pressure is not included in phase equilibrium calculations, there would not be any composition gradients for the two phase multicomponent mixture. Initially the fraction of light component (i.e. methane) in gas phase in the bulk region is smaller than in that in nanopores, and the composition of the intermediate component in oil phase (i.e. butane) is larger in bulk region compared to that in the nanopores. As shown in Figure 37 (a) and (b), diffusion decreased the composition gaps of methane in gas phase and butane in oil phase between fracture and matrix by transporting methane in gas phase from the matrix to fracture and butane from fracture to the matrix. In addition, as shown in Figure 38(c), such component migration within phases enlarges the difference of oil (gas) saturation between bulk and nano-pore region. As a result, the overall composition redistributes by diffusion and fluid properties change accordingly.

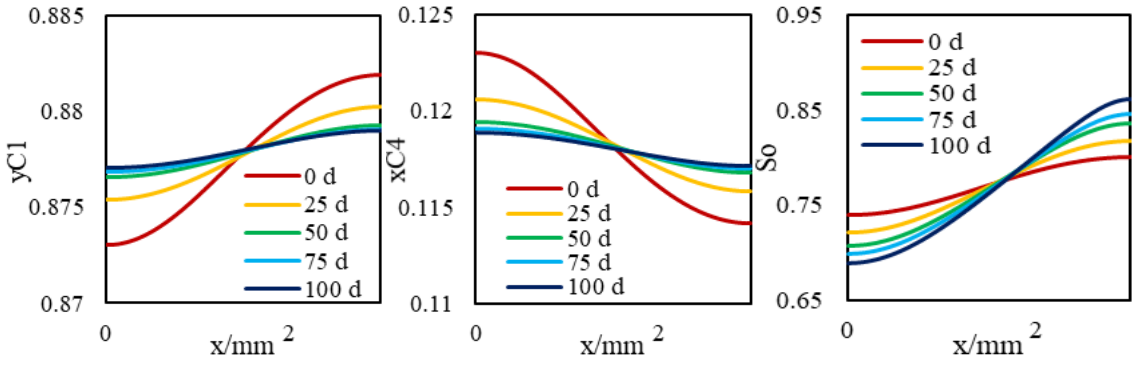

Figure 37. (a) Methane composition in gas phase (b) Butane composition in liquid phase (c) Oil saturation profile, results are without Pc in flow and with diffusion, ternary mixture

Besides the effect of inclusion of capillary pressure in phase equilibrium which causes composition gradients in heterogeneous porous media, inclusion of capillary pressure in flow also help transfer

gas from the nanopores to the bulk region. If capillary pressure in flow is considered, as shown in Figures 38, for the two models with Pc in flow (yellow and blue line, $ref = 1$), the oil pressure in fracture is higher than in matrix so that oil flows from fracture to the matrix. Meanwhile, the gas pressure is higher in nanopores (matrix) so that gas flows into the fracture until an equilibrium is achieved. Therefore, in a heterogeneous reservoir with pore size distribution, such as the fracture-matrix system, the intermediate components would likely migrate with oil phase from fracture into the matrix and light components would transport into the fracture with gas.

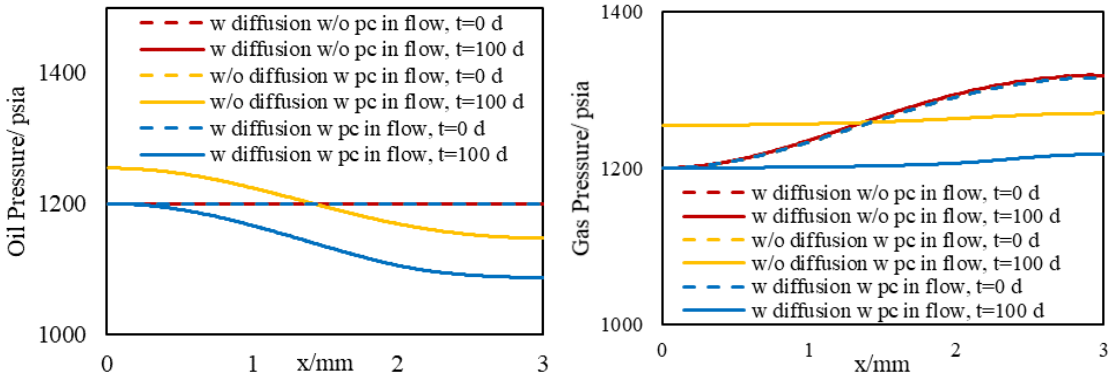

Figure 38. Oil and gas pressure distribution at initial time step (t=0d) and final time step (t=100d) for different models, ternary mixture, 1200psi

As shown in the previous results of slim tube simulations, as decrease of reservoir permeability, diffusion significantly reduces the recovery of CO_2 displacement in slim tube simulation. The composition profile with dimensionless velocity of Figure 39 points out the reason of such decrease in recovery. For CO_2 displacement, a higher and 'piston like' CO_2 front indicates higher displacement efficiency and final recovery. As shown in figure 39, as permeability decreases, the composition value of CO_2 front decreases. And the compositional gradient of CO_2 also decreases with the decrease of permeability, which neutralize the 'piston-like' displacement. Because diffusion tend to dominate Darcy's flow as permeability decrease to scale of nano-darcy and will reduce the compositional gradient of CO_2. Therefore, for ultra-low permeability reservoir, with effect of diffusion, the value of MMP increases about 200psi. For lower pressures the recovery of CO_2 displacement decreases with reduce of permeability.

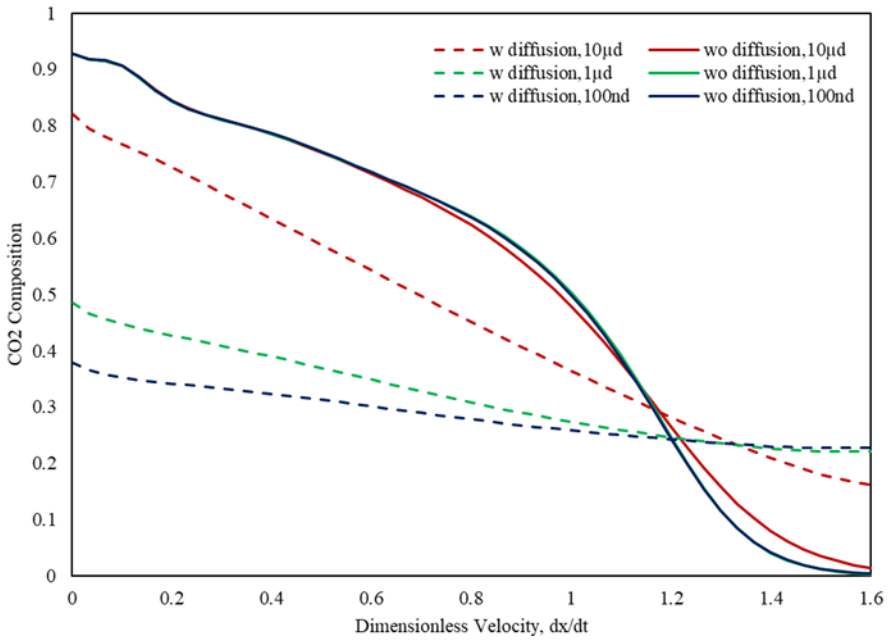

Figure 39. CO_2 composition versus dimensionless velocity with and without diffusion for different permeability, Bakken, heterogeneous pore size reservoir

In conclusion, our research suggests that within heterogeneous nano-pore size domain, such as fracture-shale matrix system, there will be a phase and overall compositions redistribution with diffusion and capillary pressure accounted for. And the diffusion mass transfer is comparable to the flow driven by capillary pressure only with ultralow permeability, on the order of nano-darcy. Otherwise, for higher permeabilities, mass transfer would be convection dominated. Therefore, diffusion must be considered in the simulation of heterogeneous shale reservoirs. For the mass redistribution, specifically, the light component tends to move to the fracture and mid-heavy components tend to accumulate in matrix and the maximum compositional change will be around 10%. Such mass transport mechanisms are valid for different shale fluids and the fluid properties will also deviate from its original values in both fracture and matrix region and the maximum difference is about 5%. For CO_2 injection, as shown from the results of 1D simulations, heterogeneous pore size reservoir rarely changes the multi-contact MMP (MCMMP) but its value increases with the decline of permeability and will meet with the value of first-contact MMP

(FCMMP) as permeability goes to zero, which means flow transport is completely dominated by diffusion.

6. Highlights

The key highlights of this research are:

- For the first time, we proposed a new drive for mass transfer of two phase oil gas multicomponent fluids in highly heterogeneous nano-porous media with pore size distribution.
- Owing to the high gas-oil capillary in nanopores, in heterogeneous porous media with pore size distribution, phase compositions are altered and different phase compositions are resulted in pores with different sizes.
- Different phase compositions in neighboring pores (or fracture and matrix) with different pore sizes result in composition gradients and this phase composition gradient is the driving force for diffusion.
- There exists selective matrix-fracture component mass transfer during both primary production and gas injection EOR.
- Such selective matrix-fracture component mass transfer is caused by diffusion while the inclusion of capillary pressure in flow will also help selective mass transfer.
- Specifically, the light components accumulate in the bulk region (or fracture) and the heavier components accumulate in the nanopore region (shale matrix). The maximum compositional change is around 10%.
- This selective component mass transfer is valid for different shale fluids and the fluid properties also deviate from original values and the maximum difference is about 5%.
- During primary recovery, diffusion is only important for ultra-tight rocks with permeabilities smaller than 1 nd.

- Heterogeneous pore size reservoir rarely changes the multi-contact MMP
- The value of MCMMP increases with permeability decreasing and will get to the value of FCMMP as mass transport is advection-free and completely diffusion-dominated (permeability equals to zero).

7. Nomenclature

P^V = *vapor pressure*

P^L = *liquid pressure*

p_c = *capillary pressure*

ref = *adjusting parameter for the reference pressure*

X_i = *parachor of component* i

q_α = *flow of phase* α

$\vec{J}_\alpha^i$ = *Fickian diffusion flow of phase* α

c_α^i = *mass fraction of component* i *in phase* α

ρ_α = *mass density of phase* α

S_α = *saturation of phase* α

D_α^i = *diffusion coefficient of component* i *in phase* α

D_{ij} = *binary diffusion coefficient between component* i *and* j

∂_α = *molar density of phase* α

$\partial_{\alpha r}$ = *reduced molar density of phase* α

M_i = *molar weight of component* i

σ_{ij} = *collision diameter*

Ω_{ij} = *collision integral of the Lennard-Jones potential*

v_{ci} = *critical volume of component* i

ω_i = *acentric factor of component* i

P_{ci} = *critical pressure of component* i

T_{ci} = *critical temperature of component* i

ε_i = *characteristic Lennard-Jones energy (ergs)*

k_B = *Boltzmann's constant*

8. Acknowledgement

The Author would like to acknowledge the contribution of Dr. Nojabaei. She provided the idea of model construction and guidance during the project. The author also would like to thank Fengshuang Du for providing support on diffusion coefficients calculation and help to polish the words.

Reference

Boyer, C.P. (2007). Producing Gas from Its Source.

Brusilovsky, A. I. (1992, February 1). Mathematical Simulation of Phase Behavior of Natural Multicomponent Systems at High Pressures With an Equation of State. Society of Petroleum Engineers. doi:10.2118/20180-PA

Cronin, M., Emami-Meybodi, H., & Johns, R. T. (2018, April 14). Diffusion-Dominated Proxy Model for Solvent Injection in Ultra-Tight Oil Reservoirs. Society of Petroleum Engineers. doi:10.2118/190305-MS

Chordia, M., & Trivedi, J. J. (2010, January 1). Diffusion in Naturally Fractured Reservoirs- A-Review. Society of Petroleum Engineers. doi:10.2118/134589-MS

Du, F.; Nojabaei, B. A Review of Gas Injection in Shale Reservoirs: Enhanced Oil/Gas Recovery Approaches and Greenhouse Gas Control. Energies 2019, 12, 2355.

Dong, Z., Holditch, S. A., McVay, D., & Ayers, W. B. (2011, January 1). Global Unconventional Gas Resource Assessments. Society of Petroleum Engineers. doi:10.2118/148365-MS

Darvish, G. R., Lindeberg, E. G. B., Holt, T., Kleppe, J., & Utne, S. A. (2006, January 1). Reservoir Conditions Laboratory Experiments of CO2 Injection into Fractured Cores. Society of Petroleum Engineers. doi:10.2118/99650-MS

Ghorayeb, K., & Firoozabadi, A. (2000, March 1). Numerical Study of Natural Convection and Diffusion in Fractured Porous Media. Society of Petroleum Engineers. doi:10.2118/51347-PA

Guillermo J. Zarragoicoechea, Victor A. Kuz, Critical shift of a confined fluid in a nanopore, Fluid Phase Equilibria, Volume 220, Issue 1, 2004, Pages 7-9, ISSN 0378-3812, https://doi.org/10.1016/j.fluid.2004.02.014.

Joachim Moortgat and Abbas Firoozabadi, Fickian Diffusion in Discrete-Fractured Media from Chemical Potential Gradients and Comparison to Experiment, Energy & Fuels 2013 27 (10), 5793-5805, DOI: 10.1021/ef401141q

King, G. E. (2010, January 1). Thirty Years of Gas Shale Fracturing: What Have We Learned? Society of Petroleum Engineers. doi:10.2118/133456-MS

Kuila, U., & Prasad, M. (2011, January 1). Understanding Pore-Structure And Permeability In Shales. Society of Petroleum Engineers. doi:10.2118/146869-MS

Ma, Y., Jin, L., & Jamili, A. (2013, September 30). Modifying van der Waals Equation of State to Consider Influence of Confinement on Phase Behavior. Society of Petroleum Engineers. doi:10.2118/166476-MS

MRST: The MATLAB Reservoir Simulation Toolbox. www.sintef.no/MRST (2018b)

K.-A. Lie. An Introduction to Reservoir Simulation Using MATLAB/GNU Octave User Guide for the MATLAB Reservoir Simulation Toolbox (MRST). Cambridge University Press, 2019. www.cambridge.org/9781108492430

Nojabaei, B., Johns, R. T., & Chu, L. (2013, July 4). Effect of Capillary Pressure on Phase Behavior in Tight Rocks and Shales. Society of Petroleum Engineers. doi:10.2118/159258-PA

B. Nojabaei, N. Siripatrachai, R.T. Johns, T. Ertekin, Effect of large gas-oil capillary pressure on production: A compositionally-extended black oil formulation, Journal of Petroleum Science and Engineering, Volume 147, 2016, Pages 317-329, ISSN 0920-4105, https://doi.org/10.1016/j.petrol.2016.05.048.

Shapiro, A. A., Potsch, K., Kristensen, J. G., & Stenby, E. H. (2000, January 1). Effect of Low Permeable Porous Media on Behavior of Gas Condensates. Society of Petroleum Engineers. doi:10.2118/65182-MS

Sudhir K. Singh, Ankit Sinha, Goutam Deo, and Jayant K. Singh. Vapor−Liquid Phase Coexistence, Critical Properties, and Surface Tension of Confined Alkanes. The Journal of Physical Chemistry C 2009 113 (17), 7170-7180 DOI: 10.1021/jp8073915

Sugata P. Tan, Mohammad Piri, Equation-of-state modeling of confined-fluid phase equilibria in nanopores, Fluid Phase Equilibria, Volume 393, 2015, Pages 48-63, ISSN 0378-3812, https://doi.org/10.1016/j.fluid.2015.02.028.

Sigmund et al. 10 and Namiot. 11 showed that the effect of surface curvature on phase behavior would not be disturbed significantly except at very high surface curvatures. Such curvatures are unlikely in hydrocarbon reservoirs

Sigmund, P. M. (1976, July 1). Prediction of Molecular Diffusion At Reservoir Conditions. Part II - Estimating the Effects Of Molecular Diffusion And Convective Mixing In Multicomponent Systems. Petroleum Society of Canada. doi:10.2118/76-03-0

Teklu, T. W., Alharthy, N., Kazemi, H., Yin, X., Graves, R. M., & AlSumaiti, A. M. (2014, August 1). Phase Behavior and Minimum Miscibility Pressure in Nanopores. Society of Petroleum Engineers. doi:10.2118/168865-PA

Wang, S., Ma, M., & Chen, S. (2016). Application of PC-SAFT Equation of State for CO2 Minimum Miscibility Pressure Prediction in Nanopores. SPE Improved Oil Recovery Conference. Tulsa, Oklahoma, USA.

Zhang, K., Liu, Q., Wang, S., Feng, D., Wu, K., Dong, X., Dong, X., Chen, S., Chen, Z. (2016). Effects of Nanoscale Pore Confinement on CO2 Displacement. SPE/AAPG/SEG Unconventional Resources Technology Conference. San Antonio, Texas, USA.

Zhang, K., Nojabaei, B., Ahmadi, K., & Johns, R. T. (2018, August 9). Minimum Miscibility Pressure Calculation for Oil Shale and Tight Reservoirs With Large Gas-Oil Capillary Pressure. Unconventional Resources Technology Conference. Houston, Texas, USA

Chapter 3 Conclusion and Highlights

Due to nanoscale pore radius of tight rocks and shales, capillary pressure is large enough to substantially influence the phase behavior and flow mechanisms of hydrocarbon fluid in shale reservoirs. Therefore, this work investigates the influence of high capillary pressure on CO_2 miscibility pressure and recovery mechanisms in heterogeneous pore size reservoir.

Our results show that capillary pressure influences MMP, however the magnitude of this change depends on the composition of the original oil, number of phases of the original oil at the MMP, and miscibility mechanisms. We confirm that the first-contact MMP is not influenced by capillary pressure as at the critical point, capillary pressure is zero. Our results suggest that the change in MMP is often negligible for practical use and often falls with 5% of the estimated MMP. One reason for this small change is that as the pressure gets close to MMP, two phases become similar (*K-values* approach unity), therefore IFT drops, and as a result, calculated capillary pressure at the equilibrium drops to a value that does not make large impact.

We also examined the effect of large gas-oil capillary pressures on the recovery efficiency of immiscible gas injection EOR and we have evidence that capillary pressure influences the effectiveness of CO_2 immiscible flood substantially for pressures well below MMP. An immiscible gas injection results in higher recoveries if the effect of capillary pressure is included in flash calculation. Note that although the MMP, which is based on oil phase pressure, does not change significantly under capillary pressure effect, the injection pressure, should be higher than the gas phase pressure in the matrix so that the required pressure gradient is provided for the gas to flow to formation.

The heterogeneous pore size distribution in reservoirs, such as natural fractures in the matrix, influences the distribution of fluid composition. The light components accumulate in the bulk region (or fracture) and the heavier components accumulate in the nano-pore region (shale matrix). Meanwhile, the fluid properties also vary in these regions. Molecular diffusion and the capillary

pressure gradient-driven convection/advection are the two important mechanisms for fluid transport.

We should note that within heterogeneous nano-pore size domain, such as fracture-shale matrix system, there will be a phase and overall compositions redistribution with diffusion and capillary pressure accounted for. And the diffusion mass transfer is comparable to the flow driven by capillary pressure only with ultralow permeability, on the order of nano-darcy. Otherwise, for higher permeabilities, mass transfer would be convection dominated. For the mass redistribution, specifically, the light component tends to move to the fracture and mid-heavy components tend to accumulate in matrix and the maximum compositional change will be around 10%. Such mass transport mechanisms are valid for different shale fluids and the fluid properties will also deviate from the original values in both fracture and matrix region and the maximum difference is about 5%. For CO_2 injection, as shown from the results of slim-tube simulations, heterogeneous pore size reservoir rarely changes the multi-contact MMP (MCMMP), however, if diffusion is included in the mass balance equation, The bend in the recovery curves occurs at higher pressures as permeability is decreases. For zero permeability, this pressure will be the same as the first contact MMP, which means mass transport is completely convection free and diffusion would be the only mass transfer mechanism.

The highlights of this thesis are listed as follow:

- Gas-oil capillary pressure in nanopores affects multi-contact MMP of the original oil mixture with 3 components and more, however, this effect is not significant in the cases we examined.
- Gas-oil capillary pressure does not affect the CO_2 MMP of a binary mixture as the only MMP is first contact.
- The effect of capillary pressure is larger if the MMP is below the original bubble-point pressure of the original oil.

- The change in MMP due to gas-oil capillary pressure does not go beyond couple of hundreds psi for the cases we examined and the reason for that is interfacial tension and subsequently capillary pressure gets smaller as the mixture gets closer to the critical region upon achieving miscibility.
- Considering the effect of gas-oil capillary pressure is important for designing immiscible gas floods.
- The results from slim tube simulation shows that capillary pressure inclusion in flash calculation slows the CO_2 front and enhances recoveries.
- For the first time, we proposed a new drive for mass transfer of two phase oil gas multicomponent fluids in highly heterogeneous nano-porous media with pore size distribution.
- Owing to the high gas-oil capillary in nanopores, in heterogeneous porous media with pore size distribution, phase compositions are altered and different phase compositions are resulted in pores with different sizes.
- Different phase compositions in neighboring pores (or fracture and matrix) with different pore sizes result in composition gradients and this phase composition gradient is the driving force for diffusion.
- There exists selective matrix-fracture component mass transfer during both primary production and gas injection EOR.
- Such selective matrix-fracture component mass transfer is caused by diffusion while the inclusion of capillary pressure in flow will also help selective mass transfer.
- Specifically, the light components accumulate in the bulk region (or fracture) and the heavier components accumulate in the nanopore region (shale matrix). The maximum compositional change is around 10%.

- This selective component mass transfer is valid for different shale fluids and the fluid properties also deviate from original values and the maximum difference is about 5%.
- During primary recovery, diffusion is only important for ultra-tight rocks with permeabilities smaller than 1 nd.
- Heterogeneous pore size reservoir rarely changes the multi-contact MMP
- Only first contact MMP is important for the diffusion-dominated systems, as above the FCMMP, recovery does not increase by increasing pressure.